# CHAPTER 13 SURFACE SUBSIDENCE

## 13.1 INTRODUCTION

In total extraction mining, which can include longwall mining and room and pillar mining with total or high extraction, a large block of coal is removed. As a result, the whole overburden is disturbed from the seam level all the way to the surface, as described in Section 7.2 (Fig. 7.2.1). Unlike other issues, such as ground control problems that affect underground miners, surface subsidence involves the general public. Therefore subsidence is not only a technical but also a public relations issue.

Surface subsidence changes surface topography. As a result, it also affects surface water and groundwater flow in some areas.

Subsidence regulations began in the late 1950s when the state of Pennsylvania enacted the pillar supporting plan to protect surface structures (State of Pennsylvania, 1957). But it was not until after the promulgation of the Surface Mining Control and Reclamation Act of 1977 (U.S. Congress, 1977b) that surface subsidence and its remediation became a part of public law in the U.S.

Accordingly, major surface subsidence research in the U.S. began in the late 1970s, and during the initial period, all subsidence theories were borrowed from those developed in Europe, especially the U.K. National Coal Board. As subsidence data accumulated, it was found that subsidence parameters for U.S. coalfields differ from those in Europe. Subsequently, subsidence prediction models pertaining to U.S. coalfields and structural damage mitigation techniques were developed in the late 1980s and early 1990s.

## 13.2 CHARACTERISTICS OF SURFACE MOVEMENT

### 13.2.1 Surface Movement Basin

During underground longwall mining, when the gob exceeds a certain size, strata movement reaches the surface and forms a low area of limited size above the gob. This is called the **subsidence basin**, or more exactly, the **movement basin**. When the seam is horizontal and the gob is rectangular in shape, the movement basin is approximately elliptical immediately above the gob (Fig. 13.2.1).

Defining the edge of the movement basin depends on the precision of the measurements. Currently, the contour line of 0.4 in. (10 mm) of subsidence is used to define the edge of the movement basin (Luo and Peng, 1997b). The maximum subsidence ($S_o$), which is generally located at the center of the basin, increases with panel (opening) width (in two-dimension across the faceline) or gob dimensions (in three-dimension). When the panel width exceeds a critical value, the maximum subsidence reaches its maximum possible value ($S_{max}$) and begins to spread rather than increase further with increasing panel width. The panel width at this time, when $S_{max}$ starts to occur, is called the **critical panel width.** When the panel width and length of a rectangular mined-out gob are less than the critical dimension, the subsidence basin formed is smaller and shallower. The panel width is then the **subcritical panel width**. Conversely, when the panel width and length of the mined-out gob are larger than the critical width, it forms a **supercritical subsidence basin** (Fig. 13.2.1), and the corresponding panel width is supercritical. According to Luo and Peng (1997c) the critical panel width, $W_c$, is linearly related to cover depth, $h$, by

$$W_c = 100 + 1.048h \tag{13.2.1}$$

which conforms with the world wide trends (Reddish et al., 1998).

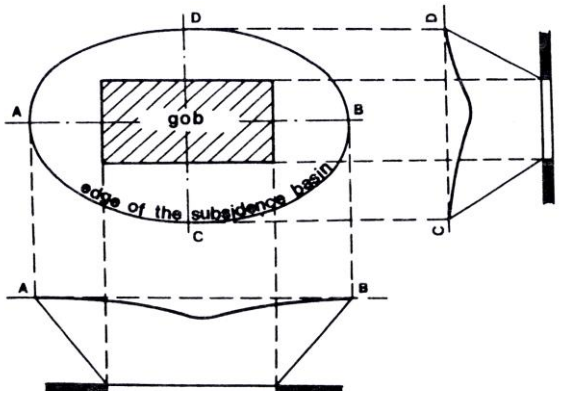


**Fig. 13.2.1 Surface subsidence basin (Peng, 1992)**

When surface subsidence due to underground mining occurs, all points, except at the panel center, move both in the vertical and horizontal directions. These are the two basic components of surface movement. But these two components vary in location and direction within a subsidence basin, causing secondary surface deformation that may be damaging to surface structures.

Surface movements and deformations consist of the following seven components (Figs.13.2.2 and 13.2.3):

1. **Subsidence, *S*** -- The vertical component of the surface movement vector is surface subsidence. When the panel is critical or supercritical in size, the maximum subsidence reached at the panel center is the maximum possible value, $S_{max}$, for that mining condition. When the panel is subcritical in size, the subsidence reached at the panel center is called maximum subsidence, $S_o$, for that mining condition, not the maximum possible value.

2. **Displacement, *U*** -- The horizontal component of the surface movement vector is surface displacement.

3. **Slope, *i*** -- The difference in surface subsidence between the two end points of a line section in the subsidence basin divided by the horizontal distance between the two points is called the surface slope of the section.

4. **Curvature, *k*** -- The difference in surface slope between two adjacent sections divided by the average length of the two sections is called surface curvature. All those that are convex are positive curvature, while those that are concave are negative curvature.

5. **Horizontal Strain, $\varepsilon$** -- Within the movement basin, the difference in horizontal displacement between any two points divided by the distance between these two points is called horizontal strain. If the distance between the two points is lengthening, it is tensile strain, which is positive. Conversely, if the distance is shortening, it is compressive strain, which is negative.

6. **Twisting, *T*** -- This is the difference in slope between two parallel line sections separated by a horizontal distance of a unit length.

7. **Shearing strain**, $\gamma$ -- This is the difference in horizontal displacement along two parallel line sections separated by a horizontal distance of a unit length.

Within the movement basin, the areas where buildings or surface structures are subjected to damage are the disturbed zones. The remaining areas, in which there is deformation but no harm is done to buildings or surface structures, are the non-disturbed zones. The critical deformations for damage to various buildings and surface structures vary with the quality of the structural elements and types of structures.

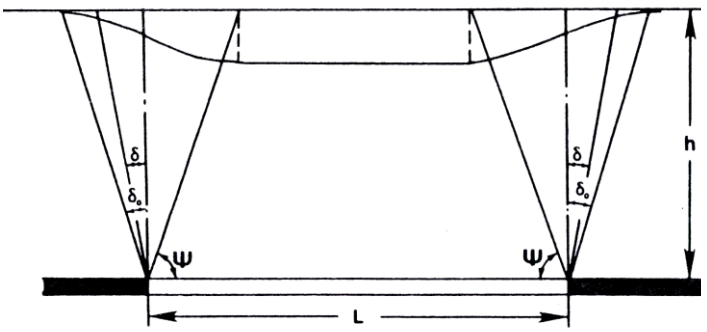


**Fig. 13.2.2 Symbols used for subsidence profile (Peng, 1992)**

The ratio of maximum possible subsidence, $S_{max}$, to mining height, $m$, is called the **subsidence factor**, $a$. The subsidence factor is a key parameter used in all subsidence prediction equations. Note that it is only applicable to cases involving critical or supercritical panel widths. For subcritical widths, it is called **apparent subsidence factor**, or $S_o/m$. The subsidence factor is also related to cover depth, $h$ by (Peng et al., 1995).

$$a = 0.6815519 \times 0.9997398^{h} \tag{13.2.2}$$

On a major cross section of the subsidence basin, which is the cross section at the center of the subsidence basin either along the mining or face line direction, the point dividing the convex and concave portions of the subsidence profile is called the **inflection point**. At the inflection point, the surface slope is at its maximum and the curvature is zero (Fig. 13.2.3). Generally, the inflection point lies above the gob edge and leans toward the gob area. The distance between the inflection point and the gob edge is the **offset distance of the inflection point**, $d$. It is also a function of cover depth, $h$, and can be determined by (Peng et al., 1995c).

$$d = 0.38123he^{-0.000699h} \tag{13.2.3}$$

When the gob has reached the critical size, or nearly so, on the major cross section of a movement basin, the angle between the vertical line at the panel edge and the line connecting the panel edge and the edge of the movement basin is the **angle of draw**, $\delta_o$ (Fig. 13.2.2). The maximum angle of draw is $24^o$ with 95 percent of it less than $20^o$. The angle of draw is fairly constant when the cover is less than 800 ft (244 m) and then increases with cover depth, $h$, such that (Peng et al., 1995c).

$$\delta_o = 27.96 - 0.02426h + 6.9 \times 10^{-6} h^2 \tag{13.2.4}$$

The angle between the vertical line at the panel edge and the line connecting the panel edge and the point of critical deformation on the surface is the **angle of critical deformation,** $\delta$ (Fig. 13.2.2). Critical deformation is the amount of deformation above which it will cause structural damage. Critical deformation depends on the type of deformation and

the types of surface structures. According to Peng et al., (1995c), $\delta$ decreases with increasing cover depth, *h*, or

$$\delta = 6.87 - 0.0072h + 8.872 \times 10^{-6} h^2 \tag{13.2.5}$$

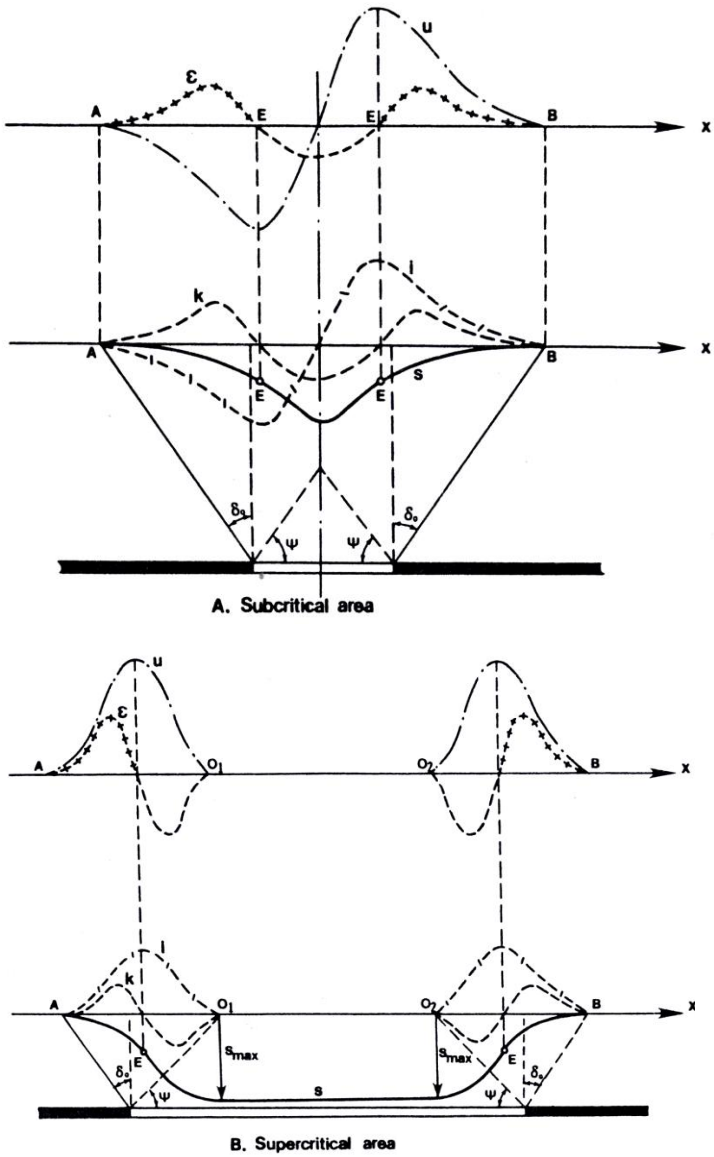


**Fig. 13.2.3 Surface movement and deformation distribution along major cross-section (Peng, 1992)**

When the gob has reached the critical size on the major cross section of the subsidence basin, the acute angle between the coal seam roofline and the line connecting the panel edge and the edge of the flat bottom of the subsidence basin is the **angle of full subsidence,** $\varphi$ (Fig. 13.2.2). It can be determined by (Peng et al., 1995c)

$$\varphi = 42.55 + 0.0417h - 2.16 \times 10^{-5} h^2 \tag{13.2.6}$$

The **angle of major influence,** $\beta$**,** is defined as the angle between the horizontal line at the mining level and the line connecting the edge of the subsidence basin and the vertically projected point of the inflection point on the coal seam. It can be determined by (Peng et al., 1995c)

$$\beta = 58.89 + 0.03089h - 1.84 \times 10^{-5} h^2 \tag{13.2.7}$$

In critical and supercritical conditions, $\beta$ can also be defined by the inflection point and the point of full subsidence.

When the gob has reached the critical size or nearly so, the elapsed time at the point of maximum possible subsidence from the initiation of surface movement to the final stabilized condition is the **movement** or **subsidence period**. The surface movement is considered to have initiated when subsidence reaches 0.4 in. (10 mm), and it is considered to have stabilized if the subsidence accumulated in six months does not exceed 1.2 in. (30 mm). The movement period is related to seam depth, rate of face advance, and overburden strata properties.

### 13.2.2 Surface Movements and Deformation during Longwall Mining

Under normal conditions, when the face has advanced for a distance approximately one-sixth to one-third of the seam depth from the set-up room, depending on the seam depth and the physical properties of the overburden strata, the movement of the overburden strata reaches the surface, whereupon the surface also begins to deform. Thereafter, the surface point where the movement initiates is always located at a fixed distance ahead of the face. The angle between the vertical line at the faceline and the line connecting the movement initiation point on the surface and the faceline is the **angle of advance influence**, *w*. The angle of advance influence can be used to determine the distance, $\ell_1$, the value of which is the influence zone ahead of the face. $\ell_1$ for the northern Appalachian coalfield can be determined by the following empirical equation

$$\ell_1 = \frac{0.113h}{1 + 0.1825\sqrt{v}} \tag{13.2.8}$$

where *v* is the face advance rate in ft/day.

Surface movement as a result of longwall mining is categorized two ways: along the faceline direction and along the mining direction.

#### 1. Along the Mining Direction

The size of the surface subsidence basin increases with the increase in gob size. In subcritical panel width conditions, the maximum subsidence in the subsidence basin increases with face advance. But when it reaches the critical panel width condition, the maximum subsidence reaches the maximum possible value and will not increase further even though the face continues to advance. Figure 13.2.4 shows the development of subsidence profiles along the face advancing direction (Wade and Conroy, 1980). The face reaches the critical condition between F and G, because before that, the maximum subsidence increases with face advance and after that the maximum subsidence does not increase any longer. It must be emphasized that all of these subsidence profiles represent the instantaneous profiles for the corresponding

face positions. If the face stops, the subsidence will increase further except for those points that have reached maximum possible subsidence. The final subsidence profile is in most cases up to 10 percent larger than the instantaneous one.

As subsidence develops following the face advance, structures on the surface tilt, rotate, and return to the original pre-mining condition except the elevation drops down by the amount of subsidence. Figure 13.2.5 shows the sequence of a house's behavior as the face advances.

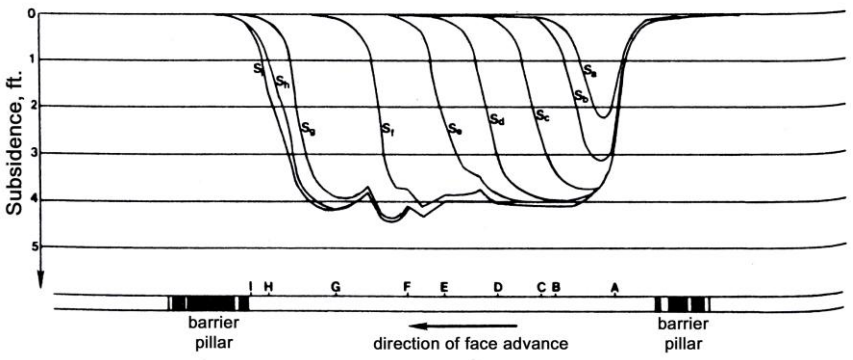


**Fig. 13.2.4 Development of a surface subsidence profile as the face advances through the panel (Peng, 1992)**

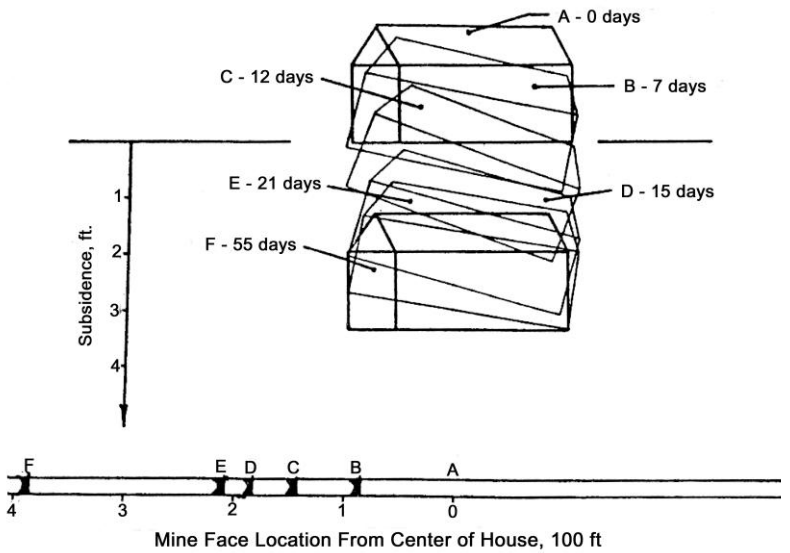


**Fig. 13.2.5 Descend of a house as the face moves (Peng, 1992)**

Whether the subsidence for a surface point has fully developed or not depends largely on face location. For instance, as shown in Fig. 13.2.6 (Peng and Cheng, 1981), when the face moves to a horizontal distance of approximately 0.8 times the seam depth, the surface at point p starts to subside. As the face moves on, the subsidence gradually increases. When the face is directly under p, the subsidence reaches only six to nine percent of the total amount of subsidence. The subsidence at p accelerates after the face has passed it. The maximum amount

of subsidence is reached and the subsidence is completed when the face has passed the point p for a distance between 1.2 and 1.7 times the seam depth.

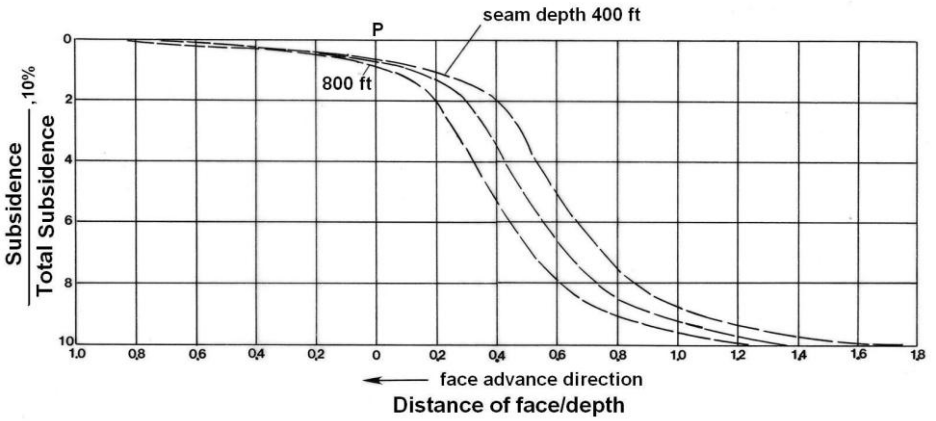


**Fig. 13.2.6 Subsidence development curve (Peng, 1992)**

Figure 13.2.6 also shows that subsidence development curves vary with seam depth. There is no significant difference before the face reaches directly under the point of interest, p, on the surface. But when the face has passed it, surface subsidence develops much faster and, thus, finishes sooner for a seam depth at 800 ft (244 m) than that at 400 ft (122 m). In other words, a shallower seam requires a relatively larger distance of face advance to reach the maximum possible subsidence than a deeper one. Subsidence development curves also change with the longwall face advancing rate (Fig. 13.2.7). The faster the face advances, the milder the subsidence development curve after the face has passed the surface point of interest. Figure 13.2.7 also shows that the effect of the face advancing rate lessens when the face is advancing more than 60 ft (18.3 m) per day.

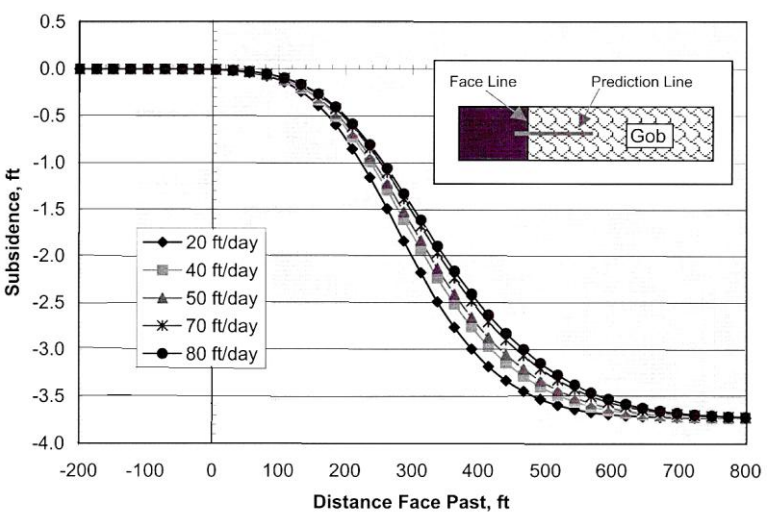


**Fig. 13.2.7 Subsidence development curves under various face advancing rates**

There are cases in which the surface ahead of the faceline heaves. The magnitude of heave is generally small. It may or may not disappear when the faceline has passed under it. Some heaving permanently remains in the final subsidence profiles.

### 2. Along the Faceline Direction

The progression of surface movements and deformations on the major cross-section perpendicular to the face advance direction (Fig. 13.2.8) differs from those parallel to the face advance direction. On the cross-section parallel to the faceline, surface movement and deformation increase gradually from small to the maximum value.

Finally, it must be noted that after the surface movement has reached the stage of full development, although there are no deformations at the flat bottom of the subsidence basin, each point there has been subjected to the sequence of progression as described above.

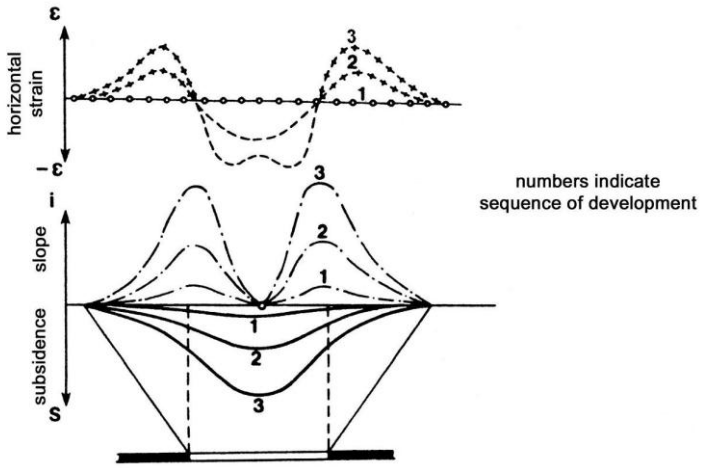


**Fig. 13.2.8 Variation of surface movements and deformations along the direction of the faceline (Peng, 1992)**

### 13.2.3 Surface Subsidence Velocity

The **subsidence velocity** differs for each point on the major cross-section of the subsidence basin. When the surface movement has not been fully developed, subsidence velocity at each point and the maximum subsidence velocity increase with an increase in the gob size. When the face advances to A or B (Fig. 13.2.9), the corresponding subsidence velocity curves are $V_a$ or $V_b$, respectively. When the gob has developed to a critical size and the surface movement is fully developed (face at C), the subsidence velocity for each surface point reaches a fixed maximum value under the prevailing conditions. Thereafter, the subsidence velocity curves are basically the same regardless of face location. The relative position of the face and the shape of the subsidence velocity curves do not change at this time. Similarly, the point where the maximum subsidence velocity occurs falls behind the face at a fixed distance and remains so. The acute angle between the seam roofline and the line connecting the point of maximum subsidence velocity and the face line is the **angle of delay**, $\phi$. The angle of delay can be used to determine the zone of most active movement during face advance.

When the face stops, the subsidence velocity for each surface point does not increase. Instead, it decreases gradually until stabilized.

The subsidence velocity reflects the movement intensity of the overburden strata above the gob area. For flat seams, when the subsidence velocity at a surface point reaches the maximum value, it indicates that the caved and the fractured zones underneath that point have reached their maximum heights.

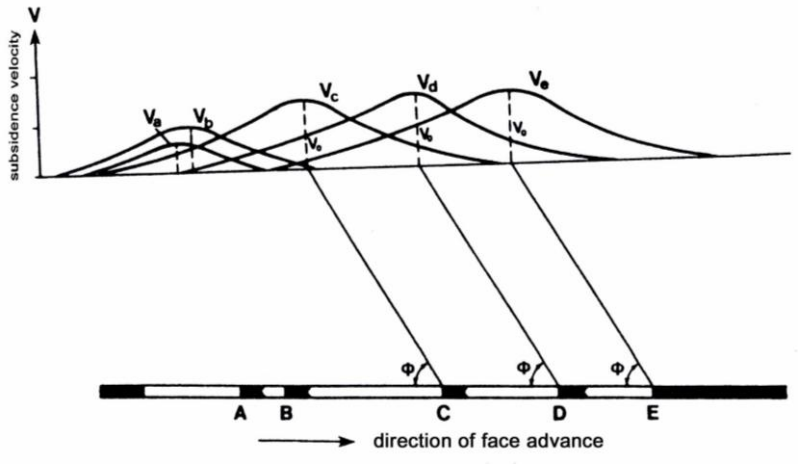


**Fig. 13.2.9 Variation of surface subsidence velocity curves as the face advances (Peng, 1992)**

## 13.3 EFFECTS OF GEOLOGICAL AND MINING FACTORS

Surface and overburden strata movements are the combined results of mining activities and geological conditions. These factors are illustrated below:

1. **Properties of the Overburden Strata** -- The physical properties of the overburden strata are some of the most important factors that control the magnitude of maximum and maximum possible subsidence. When the strata are strong and hard, the maximum or maximum possible subsidence is small. Conversely when the strata are weak and soft, the maximum or maximum possible subsidence is large.

   The shape of the subsidence profile is related to rock properties and determined by the location of the inflection point, which, in turn, varies with rock properties. When the strata are stronger, they overhang farther into the gob. As a result, the inflection point moves farther into the gob.

2. **Seam Inclination** -- Seam inclination is a very important factor that controls the characteristics of strata movement and failure. In flat and slightly inclined seams, the direction of movement is mainly perpendicular to the beddings. But, in inclined and steeply inclined seams, the direction of movement is the result of two components of movements, one is parallel and the other is perpendicular to the beddings. Also, caved rock fragments tend to slide down along the floor.

3. **Mining Depth and Mining Height** -- As mining depth increases, the area where the induced surface movements occur expands. Since the maximum subsidence in supercritical and critical panels is not related to mining depth, the surface movement basin becomes milder, and all types of deformations decrease as the mining depth increases. Thus, every other thing being equal, surface deformation is inversely proportional to mining depth.

When mining height increases, surface deformation also increases. This is why the mining-depth-to-mining-height ratio is so commonly used for determining the effects of mining conditions on surface movement. Obviously, when the depth-to-height ratio gets larger, surface deformations become smaller and milder. When the depth-to-height ratio is very small, large surface cracks, steps, and even sink holes could occur on the surface.

Mining depth affects the velocity and period of surface movement considerably. Surface movements last longer when mining depth is larger. Maximum surface subsidence velocity is inversely proportional to mining depth. When the mine is very deep, surface subsidence velocity is small and surface movement is more uniform, but it is slower and lasts longer.

4. **Gob Size** -- Before surface movement reaches the stage of full development, surface subsidence increases with an increase in gob size. The required gob size for full development of surface movement relies very much on the overburden rock properties. In order to evaluate the degree of development of surface movements, the following two development coefficients are used:

$$n_1 = C\frac{L_1}{h} \quad \text{and} \quad n_2 = C\frac{L_2}{h} \tag{13.3.1}$$

where $C$ is a rock property influence coefficient, which is larger for hard rocks. $L_1$ and $L_2$ are the length and width of the gob, respectively, and $h$ is the seam or mining depth. When $n_1 < 1$ or $n_2 < 1$, the gob is subcritical in size, and the surface movement has not reached the full development stage. When both $n_1$ and $n_2$ are larger than one, the gob is critical or supercritical in size, and the surface movement has reached the full development stage.

5. **Multiple-panel Mining** – Traditionally, mines are laid out so that there are generally two or more panels parallel to each other but separated by panel gateroads, which range from 120 to 300 ft (36.6 to 91.4 m) wide. The surface subsidence caused by one panel tends to overlap those induced by the adjacent panels if the mining height is large.

Theoretically, subsidence profiles caused by two or more panels of mining in the same neighborhood are similar to each other, and a final subsidence profile from multiple-panel mining can be obtained by simple superposition of the subsidence profile created by single-panel mining. Most multiple-panel subsidence profiles follow this principle (Fig. 13.3.1A). In practice, however, the true final subsidence may deviate considerably from that predicted by simple superposition due to variation in geological condition. Figure 13.3.1B shows the development of the final subsidence profile as a result of mining two adjacent panels (Peng and Cheng, 1981). The individual subsidence profiles for panel one and two are not similar, which is reflected in the final subsidence profile, due to various reasons such as seam depth, surface topography, and mining depth. The additional subsidence increases with the ratio of the depth to width of the chain pillar system.

6. **Faults and Other Planes of Weakness** -- Since rock in and around faults is generally much weaker than the surrounding area, shear displacements along fault planes are likely to occur in conjunction with surface subsidence process. Therefore, at the fault outcrops, strata deformation, such as cracks or even steps, is concentrated.

The intensity with which a fault controls the strata or surface movement depends on fault inclination, fault size, fault strength, and its relative position with respect to the gob.

7. **Topography** -- If there are steep slopes within the surface movement basin, its stability will be affected once the bedrock begins to move. As a result, landslides could occur on steep slopes. Generally speaking, the upper portion of the steep slope tends to slide along

the planes of weakness. If the strata bedding coincides with the steep slope, the slope will be more likely to slide along strata beddings.

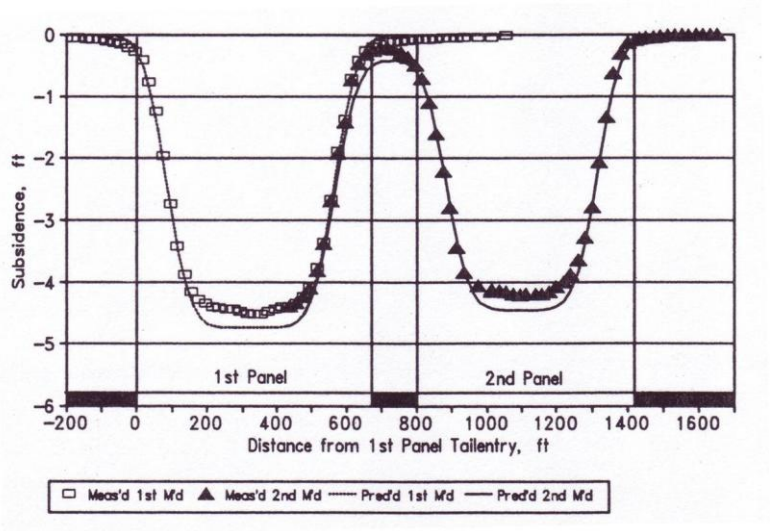


**A**

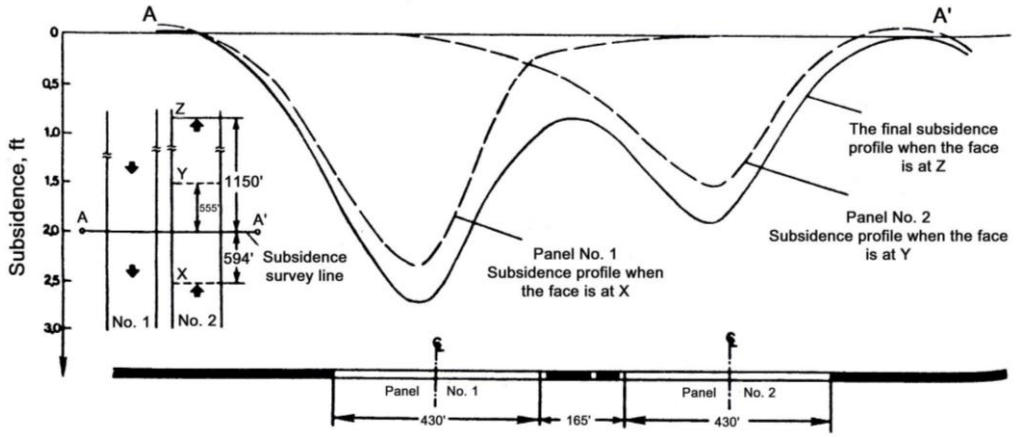


**B**

**Fig. 13.3.1 Development of surface subsidence profile in multiple-panel mining (Doney et al., 1991; Peng, 1992)**

Gentry (1977) found that subsidence was greater at topographic high points and less in areas of topographic lows due to a piling up of overburden in the low areas. When surface slope is greater than 20 % (11.3$^{o}$), horizontal displacement at the panel center will move in the direction down the dip of the surface slopes, rather than toward the panel center as in normal cases (Conroy and Gyarmaty, 1982; Khair and Molesky, 1988) (Fig. 13.3.2). Horizontal displacement up to 2 ft (0.61 m) has been recorded without slope failure. But mild slope (≤ 20 percent) has little effect on surface subsidence (Peng and Cheng, 1981).

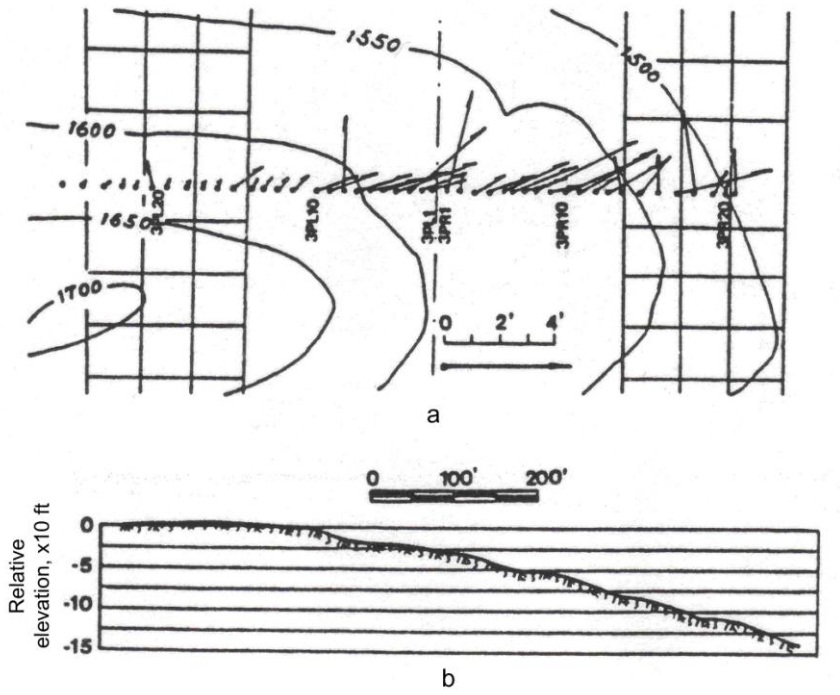


**Fig. 13.3.2 Topographic effect-surface moves downdip rather than toward panel center (Peng et al., 1987c)**

Hebblewhite et al., (2000) found evidence of large scale regional horizontal displacement of ground at great distance from active longwall panels, most of which took place toward both the river gorge and the active gob area. Maleki et al., (2000) found that escarpment shape is an important factor in escarpment stability and that convex escarpment geometry remains stable after undermining.

## 13.4 SUBSIDENCE PREDICTION METHODS

### 13.4.1 Introduction

In underground mining, prediction of potential surface subsidence is an integral part of mine design. The predicted surface subsidence can be used to assess possible subsidence influences on surface structures and environment; to improve mine design and mining methods or sequence so that the severity of the subsidence effects can be reduced; and to design and implement subsidence mitigation measures.

There are two types of subsidence predictions: dynamic and final subsidence. Dynamic subsidence is the movement of overburden strata including the surface in response to the moving longwall face, while final subsidence is the surface subsidence basin created by and long after mining has completed.

There are many methods of predicting surface subsidence (Kratzsch, 1983; Whittaker and Reddish, 1989). Most of them were developed for predicting final subsidence only and for full extraction mining methods. These methods can be classified in the following four categories: empirical methods, influence function methods, physical simulation modeling (Peng et al.,

1987a), and numerical modeling (Su, 1991). However, in this section only a few simple and more commonly used methods that are developed for U.S. coalfields will be discussed.

### 13.4.2 Empirical Methods

In empirical methods, the prediction equations or methods of prediction are based on the subsidence data collected over a particular region or regions for a period of time. Typical examples include various profile function methods and the National Coal Board's graphical method (NCB, 1975).

In this method, various mathematical functions are used to best fit the collected subsidence data.

#### 1. Negative Exponential Function Method

The negative exponential function method is more suitable for sub-critical conditions because of its asymmetrical nature about the inflection point (Peng and Cheng, 1981) (Fig. 13.4.1).

$$S(x) = S_o e^{-c\left(\frac{x}{W_s}\right)^d} \tag{13.4.1}$$

where $S_o$ is maximum subsidence, $x$ is distance from panel center, $W_s$ is the half width of subsidence basin (sub-critical and critical conditions) determined by the angle of draw, and $c$ = 8.97 and $d$ = 2.03 are coefficient.

$$W_s = \frac{W}{2} + h\tan\delta_o \tag{13.4.2}$$

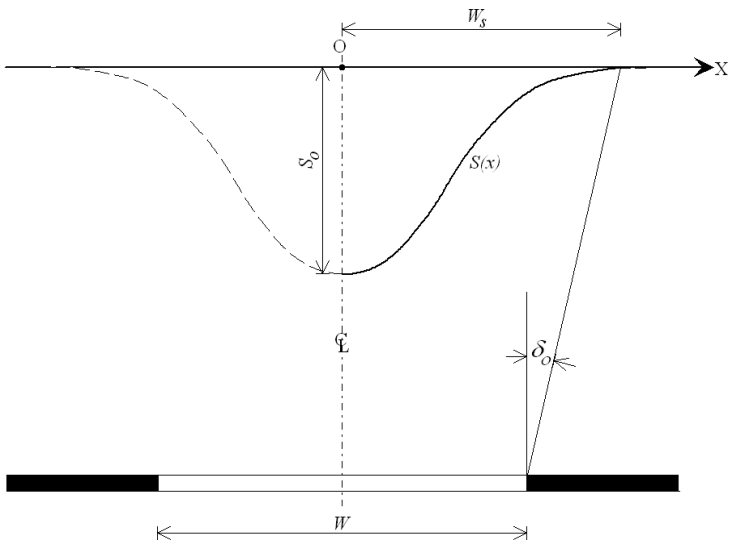


**Fig. 13.4.1 Negative exponential function (Peng and Cheng, 1981)**

#### 2. Hyperbolic Tangent Function Methods

This class of methods is more suitable for critical or super-critical conditions because of its symmetrical nature about the inflection point (Peng and Chen,1981) (Fig. 13.4.2),

$$S(x) = \frac{S_o}{2}\left[1 - \tanh\frac{cx}{h}\right] \tag{13.4.3}$$

where $c$ = 8.3 is the coefficient, $x$ is the distance from the inflection point (pointing outwards), and $h$ is overburden depth.

Another form of hyperbolic function developed by Karmis et al., (1984) is

$$S(x) = \frac{S_o}{2}\left[1 - \tanh\frac{cx}{B}\right] \tag{13.4.4}$$

where $B$ is the distance between panel center and the inflection point, $x$ is the distance from the inflection point (pointing outwards), and $c$ is a coefficient with $c$ = 1.4 for sub-critical conditions and $c$ = 1.8 for critical and super-critical conditions.

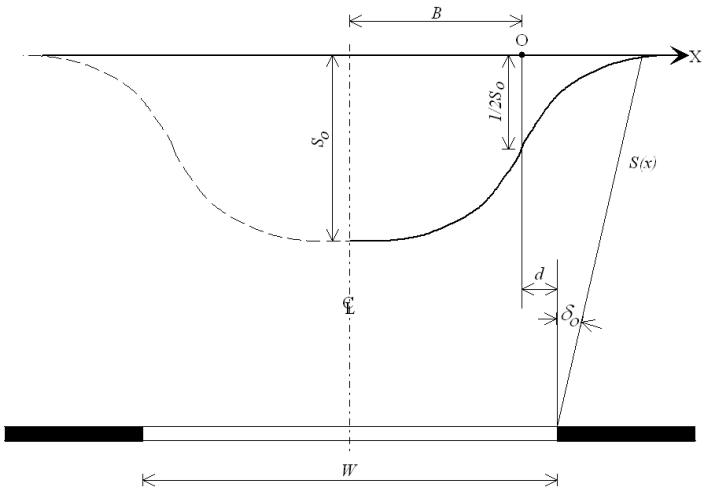


**Fig. 13.4.2 Hyperbolic tangent function (Peng and Cheng, 1981)**

Profile function methods are easy to apply, especially with manual calculations and when the parameters (coefficients) are easy to obtain, and in some cases fairly accurate. However, their application is very site specific, best suited for similar conditions of panel width, seam depth, and overburden strata; they are good for sub-critical conditions, but may not work well for super-critical conditions or vice versa; they are applicable for major cross-sections only; and deformation indices are often discontinuous at the center of the panel.

### 13.4.3 Influence Function Methods

#### 1. Influence Functions for Subsidence and Displacement

The extraction of a unit area (in plane view) of an underground coal seam will cause the surface to subside in a particular manner. Generally, the surface point located directly above the extracted unit is subjected to the largest amount of subsidence or influence. The farther the surface point is away from the extracted unit, the less subsidence or influence occurs at the surface. The mathematical function chosen to represent the distribution of the subsidence influence caused by the extraction of a unit of area is called the **influence function**.

The final subsidence at a surface point is the result of all the influences at this point when the coal seam in the mined area has been extracted unit by unit. Mathematically, the final

subsidence at a surface point is expressed as the integral of the influence function throughout the mined area.

The Knothe (1957) influence function for subsidence is (Luo, 1989; Luo and Peng, 1990b) (Fig. 13.4.3)

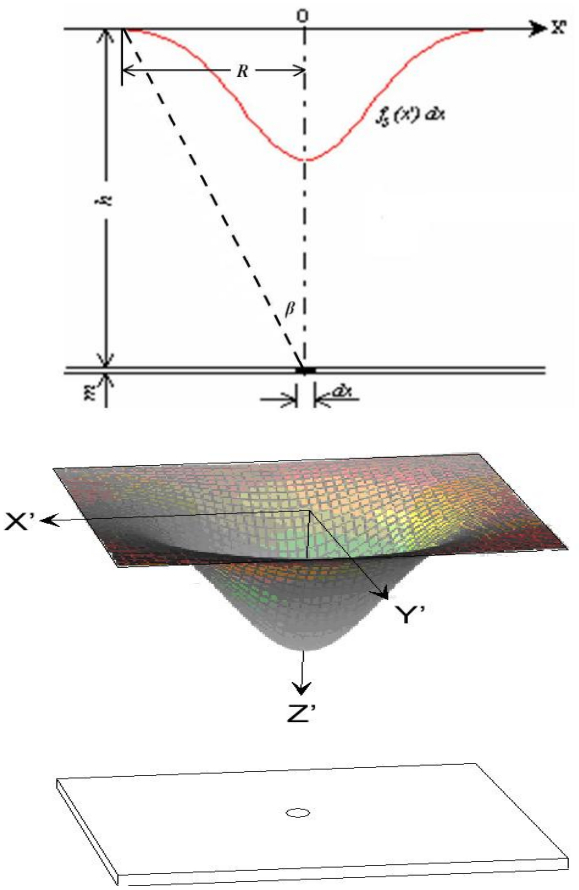


**Fig. 13.4.3 Influence function for subsidence (Luo, 1989)**

A. Subsidence

$$f_s(x',y') = \frac{S_{\max}}{R^2} e^{-\pi\left(\frac{x'^2+y'^2}{R^2}\right)} \text{ (in cartesian coordinate)} \tag{13.4.5}$$

$$f_s(\rho,\theta) = \frac{S_{\max}}{R^2} e^{-\pi\left(\frac{\rho}{R}\right)^2} \text{ (in polar coordinate)} \tag{13.4.6}$$

where $S_{max}$= $ma$ is the maximum possible subsidence, $R$ = $h$/tan $\beta$ is the radius of major influence, $x'$ is the distance between the extracted unit and the surface point where final subsidence is to be determined, $h$ is seam depth, and $\beta$ is the angle between the horizontal coal seam and the line connecting the point of interest and the limit of influence function (Fig. 13.4.3).

B. Horizontal displacement

$$f_u(\rho,\theta) = -\frac{2\pi \cdot S_{\max}}{R^2 h}\rho \cdot e^{-\pi\left(\frac{\rho}{R}\right)^2} \tag{13.4.7}$$

where $x' = \rho \cos\theta$

$y' = \rho \sin\theta$

x- component

$$f_{ux}(x',y') = -\frac{2\pi \cdot S_{\max}}{R^2 h}x' e^{-\pi\left(\frac{x'^2+y'^2}{R^2}\right)} \tag{13.4.8}$$

y- component

$$f_{uy}(x',y') = -\frac{2\pi \cdot S_{\max}}{R^2 h}y' e^{-\pi\left(\frac{x'^2+y'^2}{R^2}\right)} \tag{13.4.9}$$

## 2. Final Subsidence along a Major Cross-section

For ease of deriving the final subsidence equation from the subsidence influence function (Equation 13.4.5), a global and a local coordinate system are employed: the global coordinate O-X is set up with its origin at the left edge of a longwall panel. The X-axis is along the panel transverse direction. A local coordinate system O'-X' is set up at the point of interest or prediction point. The locations of the left- and right-side inflection points in the local coordinate are (Fig. 13.4.4)

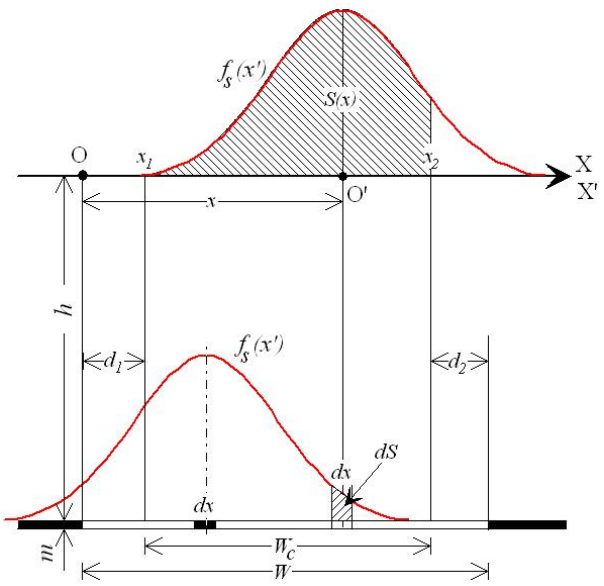


**Fig. 13.4.4 Global and local coordinate system for subsidence function (Luo, 1989)**

$$x_1' = d_1 - x \tag{13.4.10}$$

$$x_2' = W - d_2 - x \tag{13.4.11}$$

where $W$ is panel width, $d_1$ and $d_2$ are offset distances of inflection points on the left- and right-side edge of the panel, respectively, and $x$ is the point of interest. The final subsidence for the point of interest is integral to the subsidence function between the left- and right-side inflection points or through the computing width, $W_c = W - d_1 - d_2$.

$$S(x) = \frac{S_{\max}}{R}\int_{d_1-x}^{W-d_2-x} e^{-\pi\left(\frac{x'}{R}\right)^2} dx' \tag{13.4.12}$$

Similar procedures are used to obtain horizontal displacement, slope, strain, and curvature as follows:

Horizontal displacement

$$U(x) = \frac{RS_{max}}{h}\left[e^{-\pi\left(\frac{d_1-x}{R}\right)^2} - e^{-\pi\left(\frac{W-d_2-x}{R}\right)^2}\right] \tag{13.4.13}$$

Slope

$$i(x) = \frac{S_{max}}{R}\left[e^{-\pi\left(\frac{d_1-x}{R}\right)^2} - e^{-\pi\left(\frac{W-d_2-x}{R}\right)^2}\right] \tag{13.4.14}$$

Strain

$$\varepsilon(x) = \frac{2\pi S_{max}}{h}\left[\frac{d_1-x}{R}e^{-\pi\left(\frac{d_1-x}{R}\right)^2} - \frac{W-d_2-x}{R}e^{-\pi\left(\frac{W-d_2-x}{R}\right)^2}\right] \tag{13.4.15}$$

Curvature

$$k(x) = \frac{2\pi S_{max}}{R^2}\left[\frac{d_1-x}{R}e^{-\pi\left(\frac{d_1-x}{R}\right)^2} - \frac{W-d_2-x}{R}e^{-\pi\left(\frac{W-d_2-x}{R}\right)^2}\right] \tag{13.4.16}$$

## 13.5 FINAL SUBSIDENCE IN HILLY REGIONS

### 13.5.1 Introduction

It has been observed that the distribution of surface movement and deformation in steep slope areas are different from those measured in flat areas (Conroy and Gyarmaty; 1982; Khair et al., 1987b; Peng, 1986; Peng et al., 1986; Peng et al., 1987c). In particular, when the slope of the topography is larger than 20% (or 11.3$^o$), the horizontal displacement is much larger than that when the topography is flat, even though the surface subsidence component stays almost the same (O'Rourke et al., 1982; Peng et al., 1986).

### 13.5.2 Mathematical Model

The differences between surface movements on a steep slope ($S'$ and $U'$) and that on a flat surface ($S$ and $U$) are:

Incremental subsidence

$$\Delta S = S' - S \tag{13.5.1}$$

Incremental horizontal displacement

$$\Delta U = U' - U \tag{13.5.2}$$

Assuming the incremental surface movement is caused by (1) sliding of the topsoil with respect to the bedrock, and (2) surface deformation is restricted to topsoil, the unit movement, $\Delta V$, is proportional to the amount of $dV$ projected on the slope direction (Fig. 13.5.1),

$$\Delta V = G\Delta V_a = G(\sin\alpha \cdot dS + \cos\alpha \cdot dU) \tag{13.5.3}$$

where $\alpha$ is the angle of natural slope, and $G$ is a proportionality coefficient that can be expressed by (Luo and Peng, 1999)

$$G = \frac{h\gamma \sin(|2\alpha|)}{2\left[c + h\gamma \cos^2(|\alpha|)\tan\phi\right]} \tag{13.5.4}$$

where $h$ is depth of topsoil, $c$ is topsoil cohesion, $\gamma$ is unit weight of topsoil, and $\phi$ is the angle of internal friction of topsoil.

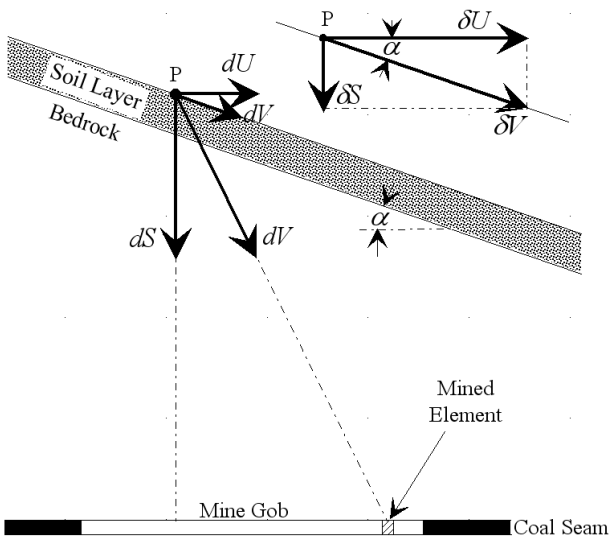


**Fig. 13.5.1 Surface movement caused by a mined unit of coal seam (Luo and Peng, 1999)**

Vertical subsidence and horizontal displacement are calculated by

A. Elemental incremental subsidence

$$\Delta S = \Delta V \sin\alpha = G\sin\beta(\sin\alpha \cdot dS + \cos\alpha \cdot dU) \tag{13.5.5}$$

B. Elemental incremental horizontal displacement

$$\Delta U = \Delta V \cos\alpha = G\cos\alpha(\sin\alpha \cdot dS + \cos\alpha \cdot dU) \tag{13.5.6}$$

C. Total unit subsidence

$$dS' = dS + \delta S = f_S'(x)\, dx \tag{13.5.7}$$

D. Total unit horizontal displacement

$$dU' = dU + \delta U = f_u'(x)\, dx \tag{13.5.8}$$

Since

$$dS = f_s(x)dx = \frac{S_{\max}}{R} e^{-\pi\left(\frac{x'}{R}\right)^2} dx' \tag{13.5.9}$$

$$dU = f_u(x)dx = \frac{2\pi \cdot S_{\max}}{hR} x' e^{-\pi\left(\frac{x'}{R}\right)^2} dx' \tag{13.5.10}$$

The influence functions are

$$f_s'(x,\alpha) = \frac{S_{\max}}{R}\left[1 + G\sin^2\alpha + G\cos\alpha\sin\alpha\,\frac{2\pi x'}{h}\right]\cdot e^{-\pi\left(\frac{x'}{R}\right)^2} \tag{13.5.11}$$

$$f_u'(x,\alpha) = \frac{S_{\max}}{R}\left[\frac{2\pi x'}{h}\left(1 + G\cos^2\alpha\right) + G\cos\alpha\sin\alpha\right]\cdot e^{-\pi\left(\frac{x'}{R}\right)^2} \tag{13.5.12}$$

The final surface movements are then

Subsidence

$$S'(x,a) = S + G\sin\alpha\left(S\cdot\sin\alpha + U\cdot\cos\alpha\right) \tag{13.5.13}$$

Horizontal displacement

$$U'(x,a) = U + G\cos\alpha\,(S\sin\alpha + U\cos\alpha) \tag{13.5.14}$$

where $S$ and $U$ are final subsidence and horizontal displacement for flat surface, respectively.

The other deformation indices are,

Slope:

$$i' = i\,(1+G\sin^2\alpha) + G\cos\alpha\sin\alpha\,\varepsilon \tag{13.5.15}$$

Strain:

$$\varepsilon' = \varepsilon\,(1+G\cos^2\alpha) + G\cos\alpha\sin\alpha\,\iota \tag{13.5.16}$$

Curvature:

$$K' = K\,(1+G\sin^2\alpha) + G\cos\alpha\sin\alpha\,d\varepsilon/dx \tag{13.5.17}$$

The final movements in subsidence basin are

A. Final Subsidence

$$S'(x,y) = C_x'\, C_y'\, S'_{max} \tag{13.5.18}$$

where
$$C_x' = S'_x(x, \alpha_x)\,/S'_{x\,max}\,(\alpha_x) \tag{13.5.19}$$
$$C_y' = S'_y(y, \alpha_y)\,/S'_{y\,max}\,(\alpha_y) \tag{13.5.20}$$
$$\alpha_x = \tan^{-1}\,(\tan\psi/\cos\psi) \tag{13.5.21}$$

$$\alpha_y = \tan^{-1}(\tan\psi / \sin\psi) \tag{13.5.22}$$

B. Horizontal displacement

$$U'_{\psi} = U_x' C_y' \cos\psi + U_y' C_x' \sin\psi \tag{13.5.23}$$

where $\psi$ is the angle between the angle of the slope direction and the x-axis.

## 13.6 FINAL SUBSIDENCE INDUCED BY CHAIN PILLARS

### 13.6.1 Introduction

U.S. longwall panels are developed with two to four entries. Since the adjacent entries are separated by chain pillars, there are 1, 2, and 3 rows of chain pillars in the 2-, 3-, and 4-entry gateroad development system. Those chain pillars are not mined during longwall retreat mining. Consequently, the movement basin created by adjacent panels may or may not overlap, depending on the overburden thickness and the strength and total width of pillars.

### 13.6.2 Mathematical Model

In determining the amount of surface subsidence over the gateroad chain pillars and their effects on the overlapping of movement basins between adjacent panels, it is assumed (Luo and Peng, 1990) that surface subsidence is related to the convergence of the chain pillar system, and that

1. The cause for additional subsidence over the chain pillars is the total convergence between the roof and the floor in the area of the chain pillar system, and consists of

$$\Delta S = \Delta S_1 + \Delta S_2 + \Delta S_3 \tag{13.6.1}$$

   where $\Delta S_1$ is the convergence due to pillars punching into roof, $\Delta S_2$ is pillar convergence, and $\Delta S_3$ is the amount of pillars punching into floor.

2. Final subsidence, $S(x)$, over and in the vicinity of the chain pillar system is the summation of the subsidence caused by mining of the individual panels, $S'(x)$, and that caused by the convergence of the chain pillar system, $S''(x)$

$$S(x) = S'(x) + S''(x) \tag{13.6.2}$$

3. The maximum possible subsidence caused by the convergence of the chain pillar system, $\Delta S_{max}$, is proportional to the total convergence of the chain pillar system.

Therefore the determination of $S(x)$ consists of the following three steps: (1) determination of $\Delta S_{max}$; (2) determination of the distribution of $S''(x)$; and (3) superposition of the subsidence caused by mining of the individual panels and that by the convergence of the chain pillar system $S'(x) + S''(x)$.

The determination of $\Delta S_{max}$ consists of the following two steps:

Step 1 Identify important factors and outline the relationship (Fig. 13.6.1)

(1) Loading index ($I_l$) – the area of the overburden strata whose weight is carried by a unit width of the chain pillar system (similar to the tributary area loading)

A. Sub-critical loading condition

$$I_l = h + \frac{W_m}{W_p}\left(h - \frac{W_m}{4\tan\alpha}\right) \qquad \text{if} \quad h \cdot \tan\alpha \geq \frac{W_m}{2} \tag{13.6.3}$$

where $\alpha = 23^o$ is the break angle, $W_p$ is the total width of gateroad chain pillar system, $W_m$ is panel width, and $h$ is seam depth.

B. Super-critical loading condition

$$I_l = h + \frac{h^2}{W_p}\tan\alpha \quad \text{if} \quad h \cdot \tan\alpha < \frac{W_m}{2} \tag{13.6.4}$$

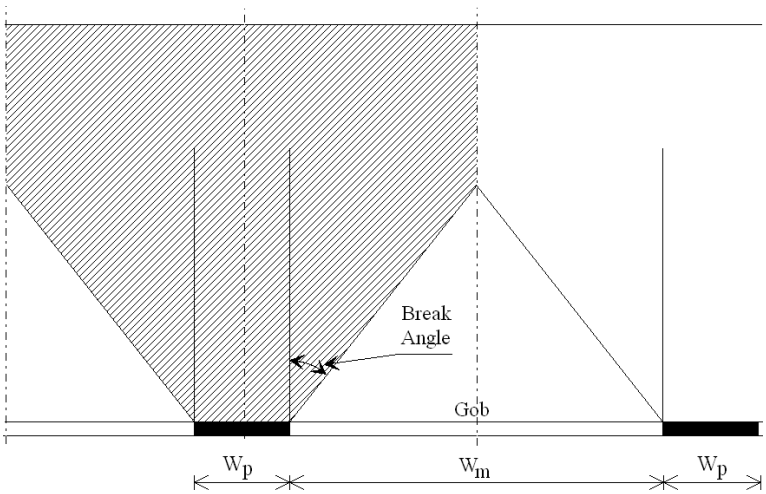


**A. Sub-critical loading**

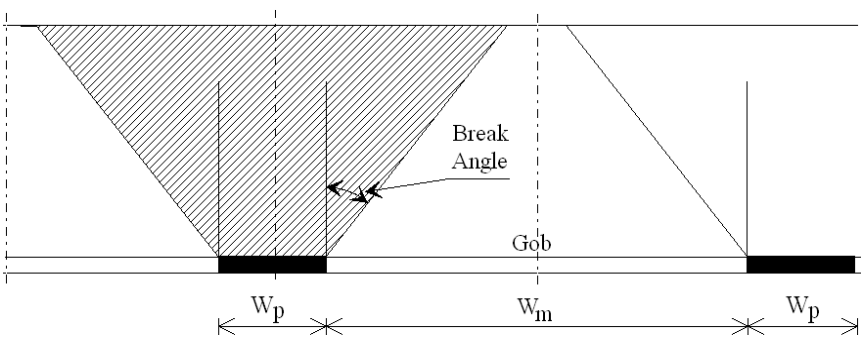


**B. Super-critical loading**

**Fig. 13.6.1 Chain pillar loading conditions**

Step 2. Distribution of subsidence caused by convergence of chain pillar system, *S''(x)*

The distribution of *S''(x)* over the chain pillar system can be determined by using the Knothe's influence function (Zhong et al., 1986) (Fig. 13.6.2),

$$S'(x) = \frac{\Delta S_{\max}}{R} \int_{x_1}^{x_2} e^{-\pi\left(\frac{x}{R}\right)^2} dx \tag{13.6.5}$$

The computing width for determining *S''(x)* is obtained by extending a distance of the offset of inflection point, *d*, from both sides of the chain pillars outward.

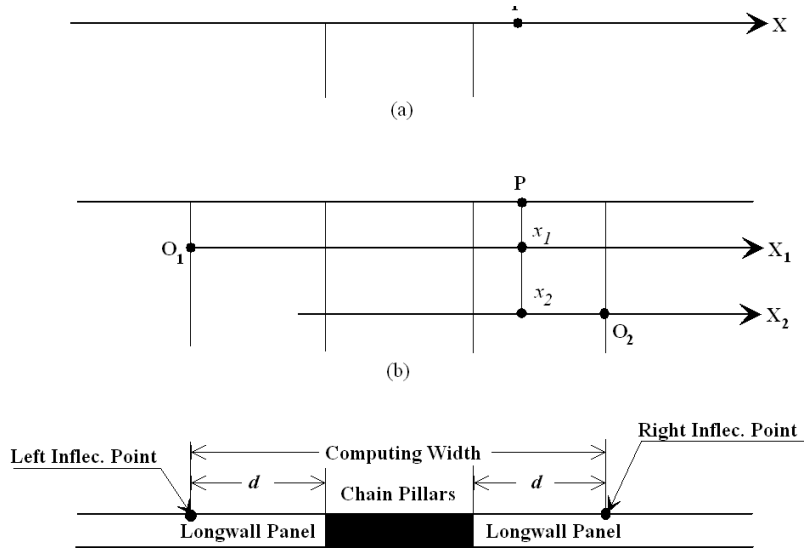


**Fig. 13.6.2 Coordinate system for predicting S''(x): (a), direct method (b), indirect method (Luo and Peng, 1990)**

## 13.7 DYNAMIC SUBSIDENCE AND SUBSIDENCE DURATION

### 13.7.1 Definition

In longwall mining, subsidence of a surface point follows the retreating longwall face. Subsidence initiates at some distance before the face arrives and continues when the face passes under it. Subsidence accelerates soon after the face passes it and then decelerates until it vanishes at some distance behind the face. This time dependent movement and deformation process of a surface point is called **dynamic subsidence**.

### 13.7.2 Phases of Dynamic Subsidence

In a longwall panel, dynamic subsidence can be divided into four phases:

1. **Subsidence initiation and development phase** $\lfloor 0 \le X_f \le (1.5-2)h \rfloor$. This phase extends from the setup room until the longwall face reaches a distance (1.5-2) times the cover depth, *h*, at which time, dynamic subsidence is fully developed under the prevailing mining condition (Stage 4 in Fig. 13.7.1A).

2. **Normal dynamic subsidence phase** $\lfloor (1.5-2)h \le X_f \le L \rfloor$: After the face has reached the point of full dynamic subsidence. Surface subsidence remains steady all the way until the face reaches the end of the panel. This is normal subsidence (Fig.13.7.1B). Note that *L* is panel length.

3. **Residual (creep) subsidence phase** ($X_f = L$ and $0 < t < \infty$): After the face has reached the end of the panel, i.e., completion of mining that panel, the time-dependent part of surface subsidence continues and normally diminishes to an insignificant amount 2-3 weeks after (Fig. 13.7.1C).

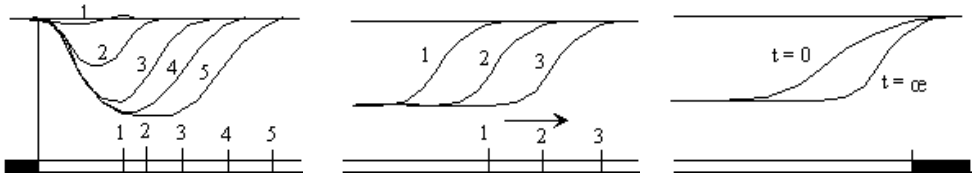


**A. Initiation Phase** **B. Normal Phase** **C. Residual Phase**

**Fig. 13.7.1 Phases of dynamic subsidence process (Luo, 2008)**

4. **Long-term subsidence** is caused by the further readjustment of overburden strata or settlement of the remnant mine structures in the mined area (particularly the chain pillar system). However experience demonstrated that this process is insignificant in most cases.

### 13.7.3 Normal Dynamic Subsidence Phase

This is one phase of the dynamic subsidence process that accounts for the great majority of longwall mining operation in a longwall panel. It is also the most well-known among the four dynamic subsidence phases. Knowledge about this phase is required for prediction of the other phases (Fig. 13.7.2).

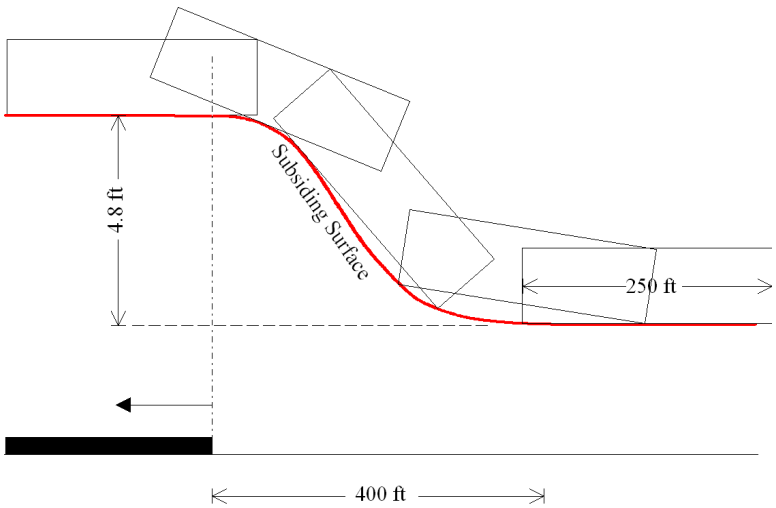


**Fig. 13.7.2 Normal subsidence development curve showing the impact of dynamic subsidence to a rectangular structure. Note that before and after the influence distance (approximately 100 ft or 30.5 m), the structure is free of subsidence effect (Luo, 2008)**

### 1. Mathematical model

It is assumed that the subsidence velocity along the longitudinal center line of a longwall panel with critical or supercritical width is a normal distribution with respect to the location of the

retreating longwall face (Peng and Luo, 1988). The subsidence distribution function is (Fig. 13.7.3)

$$V = \sqrt{\frac{2}{\pi}} \frac{V_{\max}}{\ell + \ell_1} e^{-2\left(\frac{x+\ell}{\ell+\ell_1}\right)^2} \tag{13.7.1}$$

where $V_{max}$ is the maximum possible subsidence velocity, which occurs some distance behind the retreating longwall face, $\ell$ is the distance between the longwall face and the location at which subsidence velocity is maximum, $V_{max}$, $\ell_1$ is the distance between the longwall face and the location where the subsidence could be detected for the first time, and x is the horizontal distance of the surface point of interest from the longwall face.

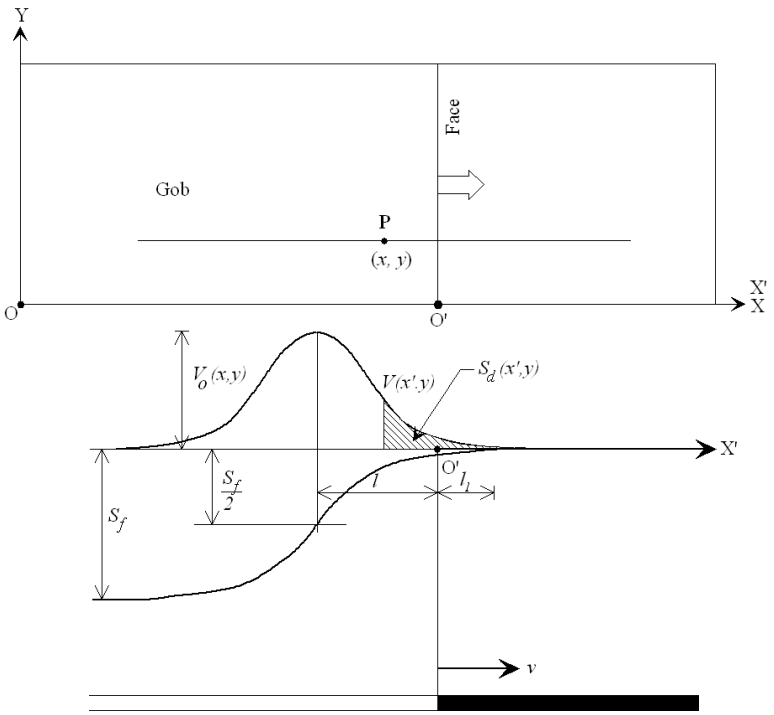


**Fig. 13.7.3 Coordinate systems for dynamic subsidence prediction (Luo, 1989)**

Regression analysis of collected dynamic subsidence data provides the following empirical equation for dynamic subsidence parameters $\ell$ and $\ell_1$

$$\ell = (2.7645 + 0.8472\sqrt{v})\sqrt{h} \tag{13.7.2}$$

$$\ell_1 = \frac{0.113h}{1 + 0.1825\sqrt{v}} \tag{13.7.3}$$

where $h$ is cover depth and $v$ is the average advance rate of the longwall face, ft/day

**2. Normal dynamic subsidence at the prediction point**

Subsidence at the prediction point is the accumulation of the incremental subsidence received up to the time of interest. In Equation 13.7.4, $x_p$ is the coordinate of the prediction point in relation to the location of the longwall face.

$$S_d(x',y)=\frac{1}{2}S_f(x,y)+\sqrt{\frac{2}{\pi}}\frac{S_f(x,y)}{l+l_1}\int_{x_p}^{-l}e^{-2\left(\frac{x'+l}{l+l_1}\right)^2}dx' \tag{13.7.4}$$

The second term can be evaluated using numerical integration techniques.

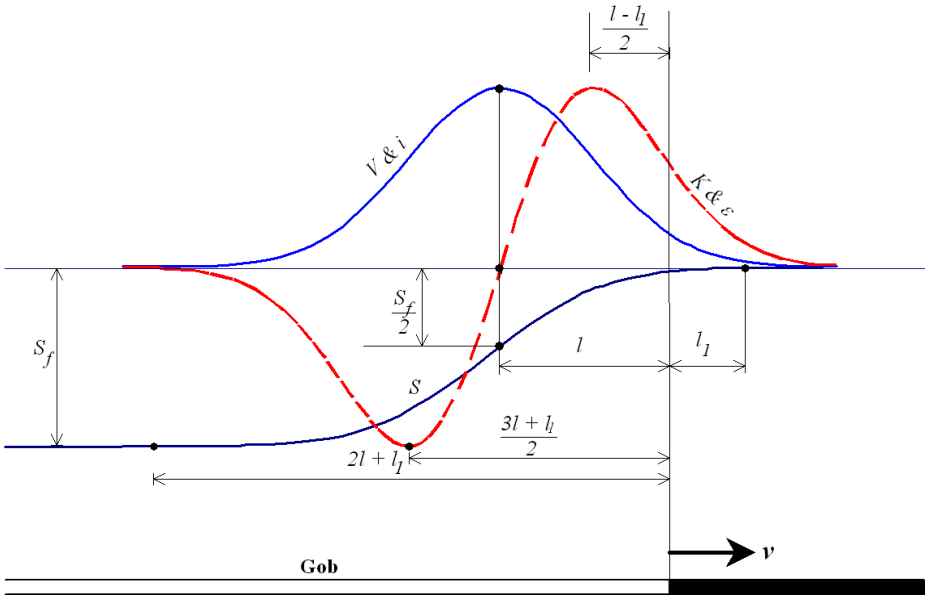


**Fig. 13.7.4 Spatial relationships among the dynamic velocity, subsidence, slope, horizontal displacement, strain, and curvature (Luo, 1989)**

### 3. Normal dynamic slope

$$i_d(x',y)=\frac{dS_d}{dx'}=-\sqrt{\frac{2}{\pi}}\frac{S_f(x,y)}{l+l_1}e^{-2\left(\frac{x'+l}{l+l_1}\right)^2} \tag{13.7.5}$$

### 4. Normal dynamic subsidence velocity

$$V(x',y)=\sqrt{\frac{2}{\pi}}\frac{v\cdot S_f(x,y)}{l+l_1}e^{-2\left(\frac{x'+l}{l+l_1}\right)^2} \tag{13.7.6}$$

Dynamic slope has the same distribution as the dynamic subsidence velocity. At the time of peak subsidence velocity, the dynamic surface slope is also at the maximum.

### 5. Normal dynamic horizontal displacement

$$U_d(x',y)=\frac{R^2}{h}\cdot i_d(x',y) \tag{13.7.7}$$

### 6. Normal dynamic curvature

$$K_d(x'y)=\frac{d^2S_d}{dx'^2}=4\sqrt{\frac{2}{\pi}}\frac{S_f(x,y)}{(l+l_1)^3}(x'+l)e^{-2\left(\frac{x'+l}{l+l_1}\right)^2}=-4\frac{x'+l}{(l+l_1)^2}\cdot i_d(x',y) \tag{13.7.8}$$

**7. Normal dynamic strain**

$$\varepsilon_d(x', y) = \frac{R^2}{h} \cdot K_d(x', y) \tag{13.7.9}$$

**8. Duration of active dynamic subsidence**

The active subsidence period is the time from which a surface point has subsided about 2% to that when it has subsided 98% of its final subsidence. Therefore it covers a distance of face travel from x' = $\ell_1$ and x' = -$(2\ell + \ell_1)$, or

$$T = 2\frac{\ell + \ell_1}{v} \text{ (day)} \tag{13.7.10}$$

Figure 13.7.5 shows the distance behind the longwall face required to reach 97.7% of final subsidence under various face retreating rates and cover depths. It shows the larger the cover depth and the faster the face advance rate, the longer the distance required.

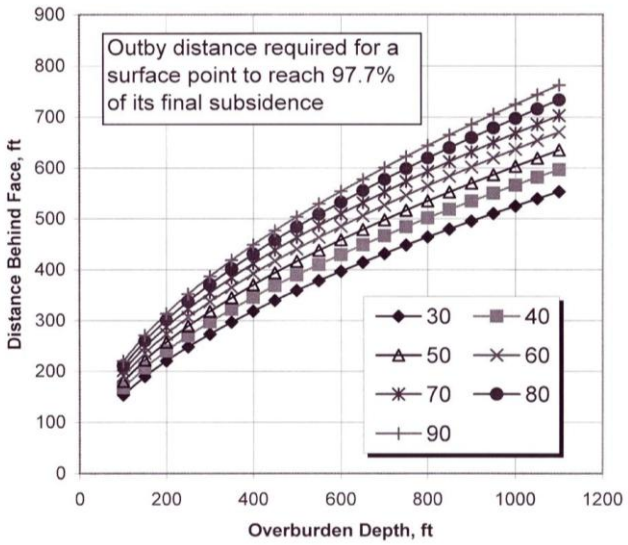


**Fig. 13.7.5 Distance behind the longwall face required to reach 97.7% of final subsidence under various face retreating face rate and cover depth**

The required distance divided by the face advance rate will be the time in days required to reach the final subsidence.

### 13.7.4 Subsidence Initiation Phase

The subsidence initiation phase can be divided into the following two stages:

**1. Stage I**

This stage occurs before the longwall face reaches the subsidence initiation distance, $L_i$ and during this period there is no or very little subsidence. The subsidence initiation distance is empirically determined by

$$L_i = 32.97 + 12.43\sqrt{h} \tag{13.7.11}$$

when $X_f = L_i$, $t = 0$ and $S = S_o$. $S_o$ is often negligible.

**2. Stage II**

This stage covers the period from when the longwall face is moving between the subsidence initiation distance and 1.5 to 2 times the overburden depth, i.e., $L_i < X_f < (1.5 \sim 2)$ h away from the panel setup entry – one of the most critical times for a longwall mining operation. Assuming that subsidence velocity at a surface point is proportional to the difference between the potential subsidence and the actual subsidence at this point, then (Fig. 13.7.6)

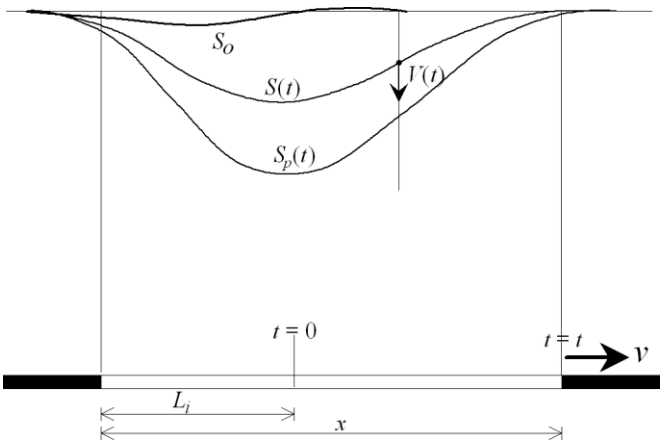


**Fig. 13.7.6 Dynamic subsidence in the initiation process (Luo, 2008)**

$$V(t) = \frac{dS(t)}{dt} = c\left[S_p - S(t)\right] \tag{13.7.12}$$

The general solution for Equation 13.7.12 is

$$\frac{dS(t)}{S_p - S(t)} = c \cdot dt \tag{13.7.13}$$

Integrating Equation 13.7.13 with respect to $t$,

$$\ln\left[S_p - S(t)\right] = -c \cdot t + D_1 \tag{13.7.14}$$

With the initial condition of $S\ (t = 0) = S_o \approx 0$, the particular solution becomes,

$$S(t) = S_p - D_2 e^{-c \cdot t} \tag{13.7.15}$$

In Equation 13.7.15, potential subsidence $(S_p)$ can be calculated using Equation 13.7.4. The coefficient $c$ is called the overburden creep factor and is determined by

$$c = \frac{2 \times 10^5}{h^{2.17}} \tag{13.7.16}$$

### 13.7.5 Residual (Creep) Subsidence

Residual subsidence occurs after a longwall face has stopped moving. This process represents a transition from the normal dynamic subsidence basin at the time immediately after the longwall face stops to the final subsidence basin formed long after mining (Fig. 13.7.7).

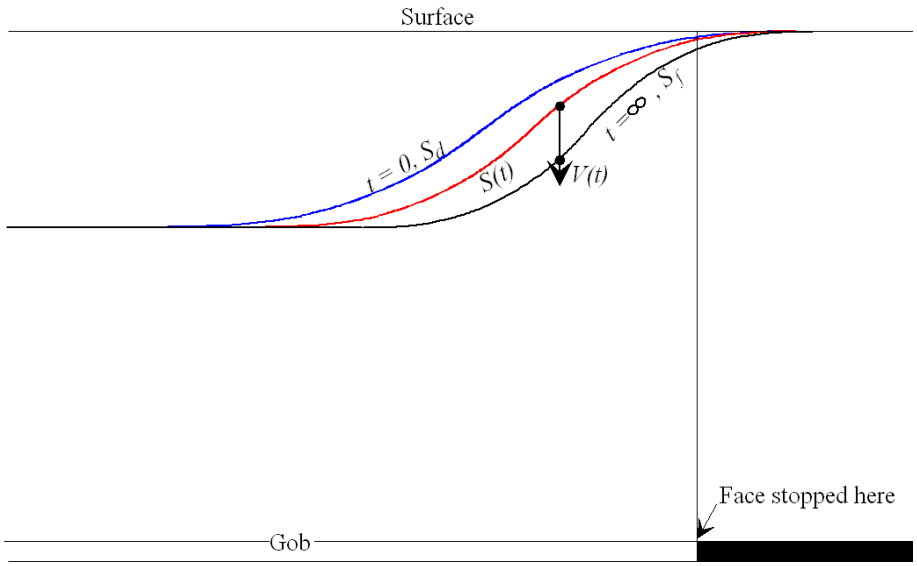


**Fig. 13.7.7 Model for residual subsidence (Luo, 2008)**

Assuming subsidence velocity at a surface point at a given time is proportional to the expected amount of subsidence (i.e., the difference between the final subsidence and the actual subsidence) for the point at the time, then,

$$V(t) = \frac{dS(t)}{dt} = c \cdot \left[ S_f - S(t) \right] \tag{13.7.17}$$

With the initial condition, $S(t = 0) = S_d$, solving for Equation 13.7.17

$$S(t) = S_f - \left( S_f - S_d \right) e^{-ct} \tag{13.7.18}$$

With the total residual subsidence, $S_r = (S_f - S_d)$, the duration of the residual subsidence process is

$$T_r = -\frac{1}{c} \ln \frac{S_f - S(t)}{S_r} \tag{13.7.19}$$

The duration of the residual subsidence phase, depending on the definition of degree of stabilization (e.g., 95% or 99% of residual subsidence), is shown in Fig. 13.7.8.

## 13.8 LONG-TERM SUBSIDENCE

As shown in Figs. 13.2.6 and 13.2.7, a surface point does not begin to subside until the longwall face has reached a certain distance inby the surface point. Thereafter, the subsidence process accelerates. The subsidence phase ends when the movement at a surface point practically stops with indistinguishable changes in subsidence measured over a normal survey interval, i.e., the subsidence reaches its quasi-stable state. The total distance for a longwall face to travel under a surface point until this surface point experiences the steady-state subsidence process is called the **normal subsidence duration**. The subsidence process at a surface point reaches its quasi-stable state when the longwall face has passed this point by a distance between 0.7 and 0.94 times the overburden depth.

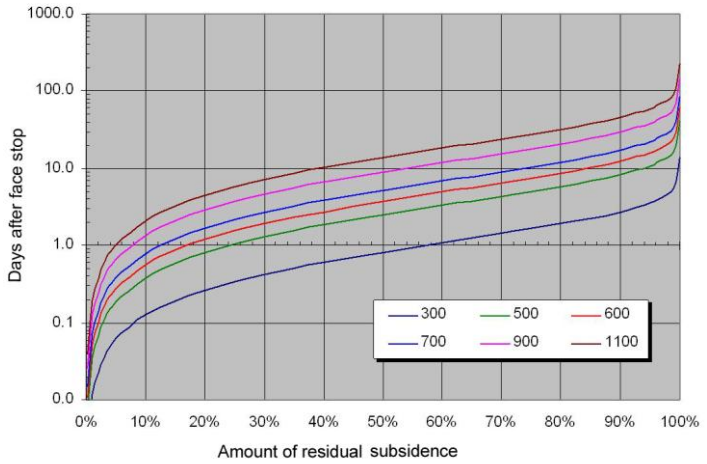


**Fig. 13.7.8 The residual subsidence period varies with cover depth (Luo, 2008) (see color figure in Appendix 3)**

After the quasi-stable state of subsidence is reached, a long-term subsidence process may follow. The **maximum long-term subsidence** at a surface point is defined to be the difference between the ultimate final subsidence ($S_u$) and the subsidence measured when the quasi-stable state is reached (quasi-final subsidence, $S_q$) at the same point. The process for a surface point to subside from $S_q$ to $S_u$ is called the long-term subsidence process, which may be due to: (1) recompaction of overburden materials in the caved and fractured zones at the panel center, and (2) creep deformation of chain pillars over the gateroads.

For long-term subsidence over the chain pillars, Luo and Peng (2000b) developed the following equations;

$$S(t) = S_q + A\left(1 - \frac{S_q}{0.65m}\right)^6 \left(1 - e^{-dt}\right) \tag{13.8.1}$$

where $S(t)$ is subsidence at time $t$, $m$ is mining height, $A$ = 2.4 is a coefficient, and $c$ is the decaying coefficient that can be obtained as

$$d = 0.001548 e^{\frac{-\eta}{\sqrt{1 - \frac{S_q}{0.65m}}}} \tag{13.8.2}$$

where $\eta < 3$, is a coefficient.

Based on Equation 13.8.1, the ultimate final subsidence ranges from zero to a significant amount. However, it takes a long time for a surface point to even reach half of the maximum long-term subsidence. The surface deformations generated in such a slow process are too small to cause any problems to surface structures.

## 13.9 SUBSIDENCE PREDICTION SOFTWARE

As illustrated in Sections 13.4 through Section 13.7, subsidence prediction is a lengthy and complicated process. For convenience of application, software has been developed (Luo and Peng, 1989; Karmis et al., 2008).

Based on the principles of influence function, an integrated and comprehensive subsidence prediction system has been developed by Luo and Peng (1989 and 1990b). The system consists of a number of mathematical models and empirical formulae and improvement mechanisms for the subsidence parameters. Based on the developed prediction system, a computer program package, CISPM, has been developed. This program has found numerous applications in all parts of U.S. coalfields and other major coal producing countries. Figure 13.9.1 shows the major components and system capability (Luo, 2008).

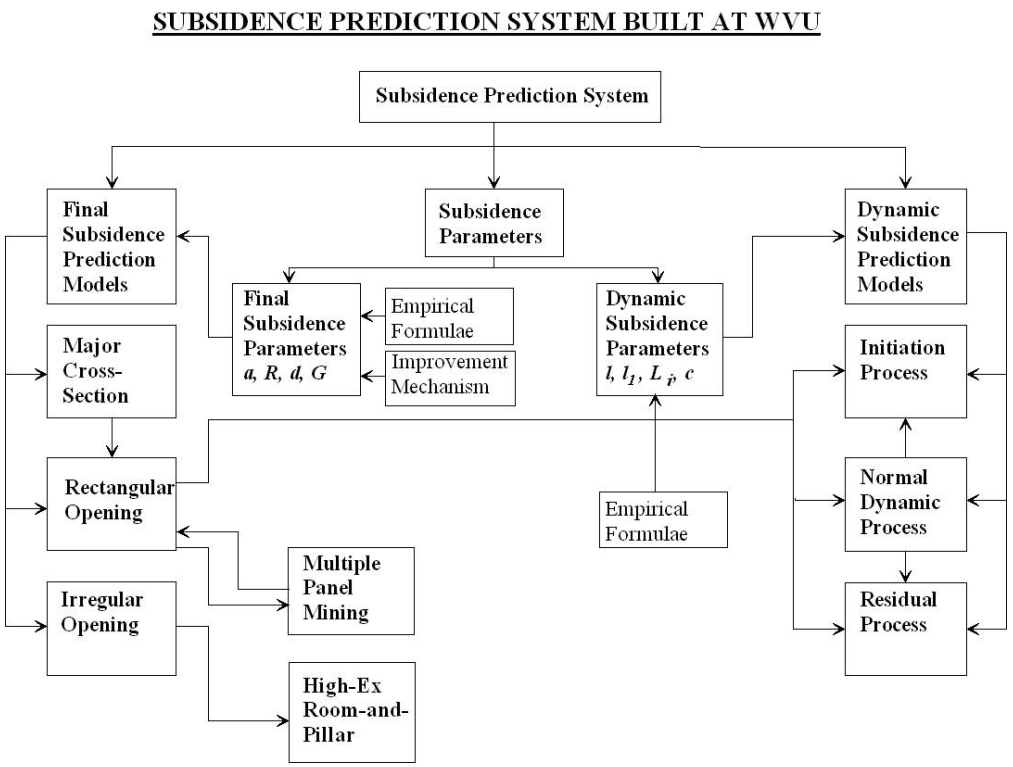


**Fig. 13.9.1 Components of CISPM (Luo, 2008)**

Another program, SDPS, employs the same influence functions and has similar features and capability for prediction of surface movements (Karmis et al., 2008). A case example of final and dynamic subsidence prediction versus the measured subsidence for both programs is shown below.

A longwall mine, 750 ft (228.7 m) deep, has two longwall panels 1,433 ft (436.9 m) wide by 19,600 ft (5,975.6 m) long separated by a three-entry system 200 ft (61 m) wide (Fig. 13.9.2). The entries and crosscuts are 16 ft (4.9 m) wide and mining height is 6.5 ft (1.98 m). The overburden contains 10% of hard rock strata. Figure 13.9.3 shows the dynamic subsidence development curves for two surface points located at the panel center. Figure 13.9.4 shows the predicted and measured final surface subsidence profiles when the first panel mining was completed. Figure 13.9.5 shows the predicted surface subsidence profiles across the two panels along the faceline direction.

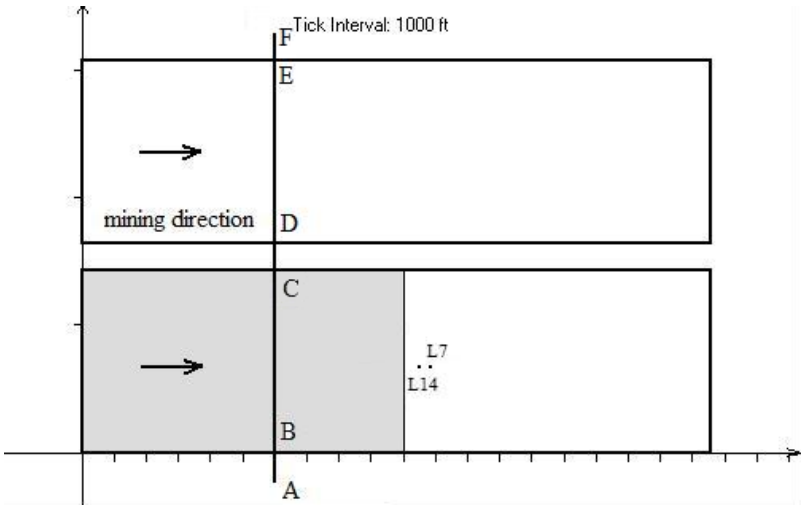


**Fig. 13.9.2 Panel layout for surface subsidence prediction**

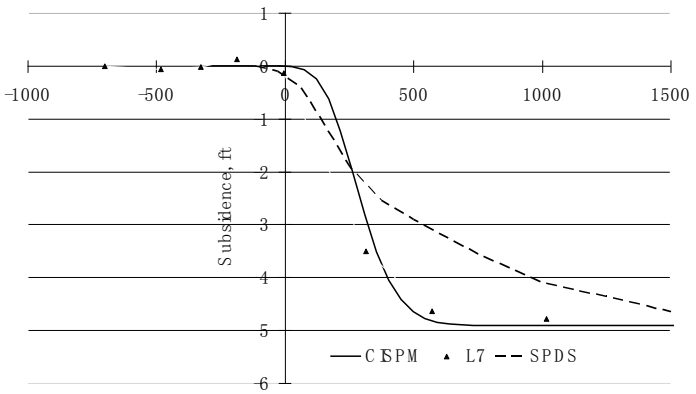


L7

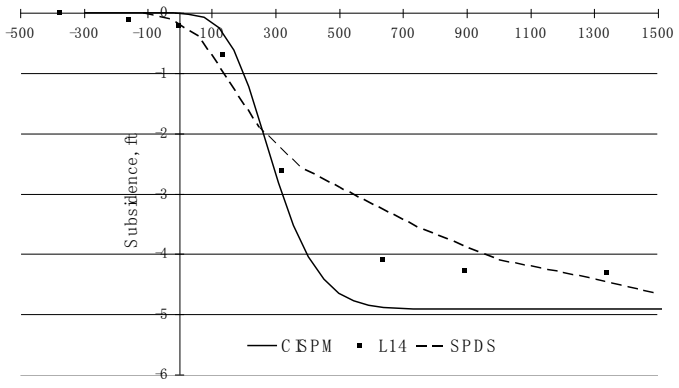


L14

**Fig. 13.9.3 Dynamic subsidence prediction for two surface points**

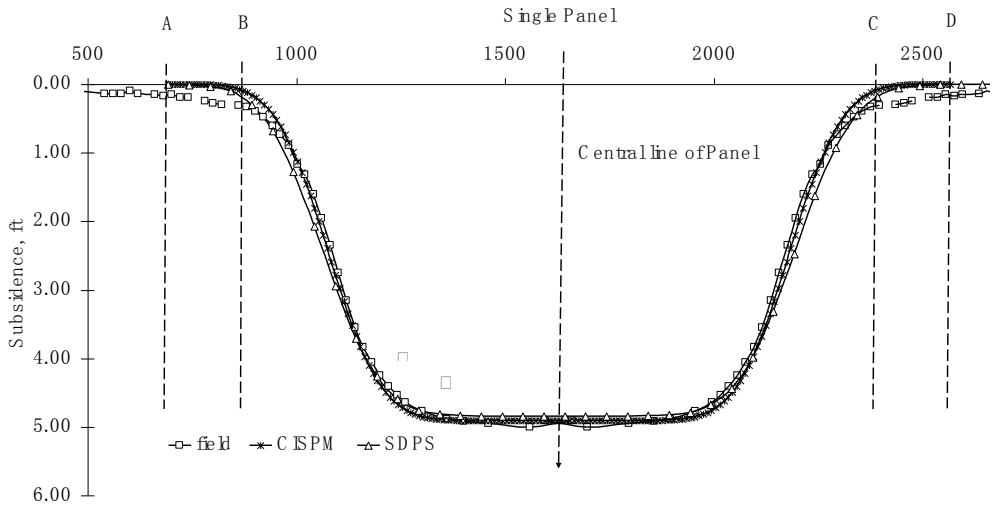


**Fig. 13.9.4 Predicted and measured subsidence profiles for single panel mining**

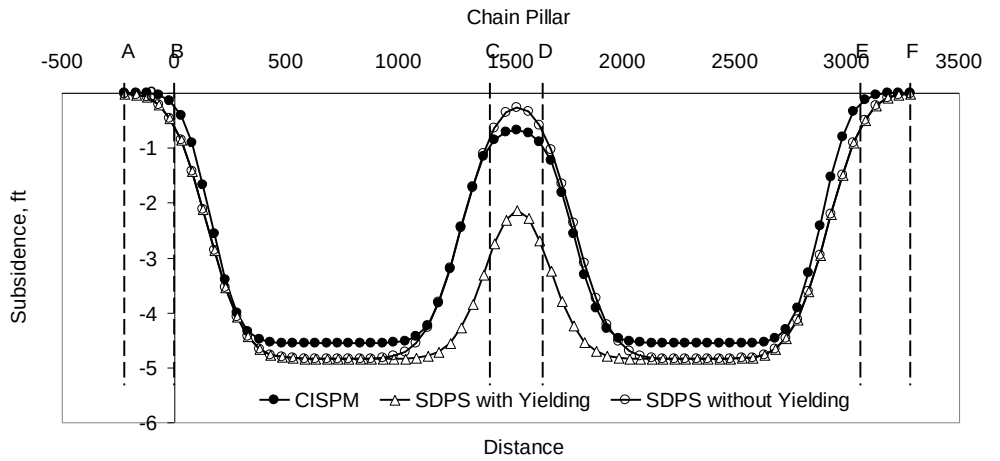


**Fig. 13.9.5 Predicted surface subsidence profiles for two adjacent panels across AF cross-section in Fig. 13.9.2**

## 13.10 SURFACE SUBSIDENCE MONITORING

### 13.10.1 Introduction

Surface subsidence monitoring is often required in order to validate and refine the subsidence prediction models used or, in case of virgin ground, to provide data for development of site specific prediction models.

Surface subsidence monitoring consists of the following tasks: (1) selection and layout of subsidence monuments, (2) survey methods and instruments, (3) survey frequency and duration, and (4) data processing.

### 13.10.2 Selection and Layout of Subsidence Monuments

A **monument** is a specially-constructed station for surface subsidence surveying. Various types of monuments have been used including, in order of sophistication, paint marks on the ground, wood or steel rods, concrete grouted steel bars (Fig. 13.10.1), and weather-proof monuments (Fig. 13.10.2). Except the paint mark method, the depth of insertion into ground ranges from 1.5 ft to 5 ft (0.46 to 1.5 m) below the surface.

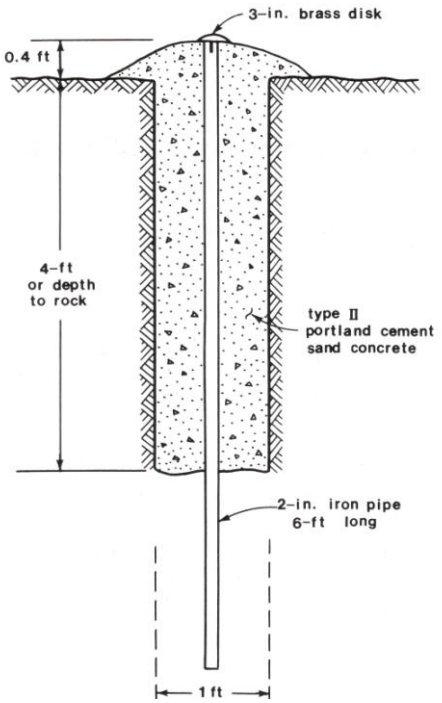


**Fig. 13.10.1 Monument constructed with concrete and rebar (O'Rourke et al., 1982)**

The criteria for monument selection include required accuracy, monitoring duration, weather conditions (e.g., large temperature variation, freezing and thawing), tamper proofing, ease of installation and removal, conditions imposed by the land owner, and time required in each survey.

The monument distribution patterns also vary from a few stations at strategic points to a full grid pattern (Fig. 13.10.3): (1) a grid pattern to cover the whole or parts of the area of interest, (2) a full profile along the face line and/or the face retreat direction, (3) one-half profile along the face line and/or the face retreating direction, and (4) evenly or unevenly spaced monuments (e.g., denser in areas of greater concern). The full or half profile is the most common types and they are normally placed at the center of the longwall panel to avoid the panel edge effect. To evaluate the effect of panel corners, a $45^{o}$ diagonal line of monuments has been used.

Monument spacing should be determined based on the application of data acquired. For determination of subsidence parameters, spacing should be as dense as practically allowed. For determination of deformation indices, monument spacing should depend on the relative error allowed in the derived deformation indices.

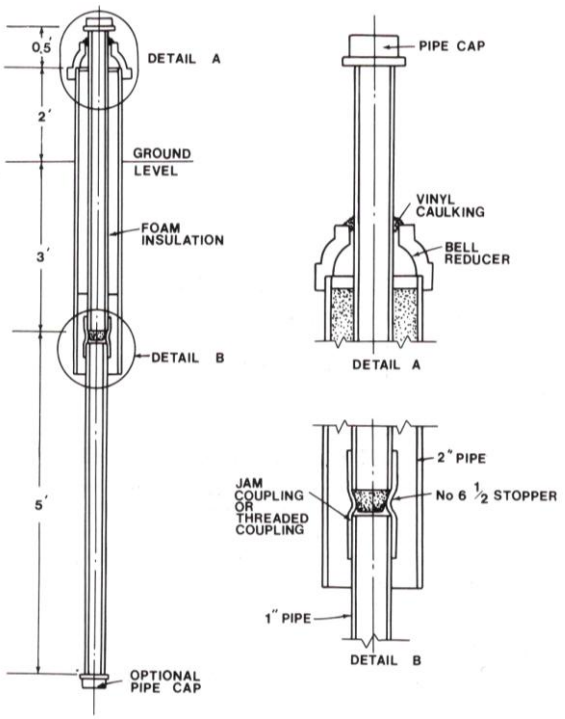


**Fig. 13.10.2 Monument with double tubing to eliminate freezing and thawing effects (Conroy and Gyarmaty, 1983)**

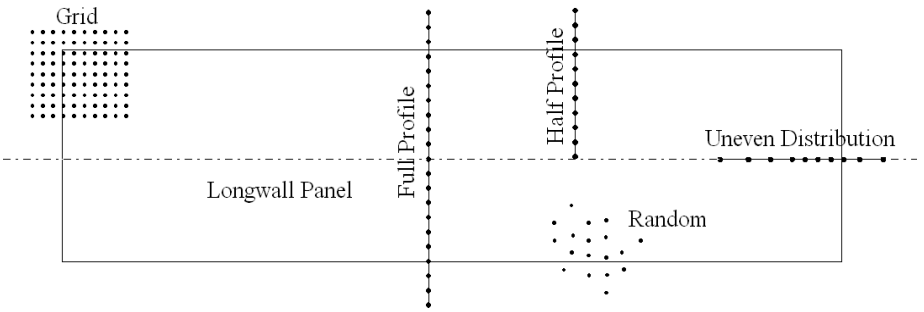


**Fig. 13.10.3 Various monument layout patterns and spacing**

For example, monument spacing can be determined based on the required limit of relative error. Relative error in strain is derived from the measured horizontal displacement, *U'*, which is a combination of the true movement, *U*, and a measurement error, $\Delta U$,

$$U' = U \pm \Delta U \tag{13.10.1}$$

Strain:

$$\varepsilon' = \frac{U'_{i+1} - U'_i}{\Delta x} = \frac{U_{i+1} - U_i}{\Delta x} \pm \frac{\Delta U_{i+1} - \Delta U_i}{\Delta x} = \varepsilon \pm \Delta\varepsilon \tag{13.10.2}$$

For smaller spacing, accuracy of $\varepsilon$ will increase, but $\Delta\varepsilon$ will also increase. Relative error in the derived strain is

$$e_{\varepsilon} = \left| \frac{\Delta\varepsilon}{\varepsilon} \right| \tag{13.10.3}$$

Therefore, proper monument spacing should consider:

1. $\Delta x$ = (0.1 ~ 0.2) h, where $\Delta x$ is monument spacing and h is cover depth,
2. No fewer than 20 points for a full profile, and
3. The required survey time to complete a full survey should be such that during the survey period additional subsidence would be insignificant.

### 13.10.3 Survey Methods and Instruments

A surface subsidence survey employs the same principles as the conventional land survey, and as such, all equipment is applicable, including

1. level – to measure subsidence only
2. Transit – to measure both subsidence and horizontal displacement
3. Electronic distance meter (EDM) – to measure horizontal displacement only
4. Auto level and EDM assembly - to measure both subsidence and horizontal displacement (Fig. 13.10.4)
5. Electronic total station – to measure both subsidence and horizontal displacement with fairly good accuracy (Fig. 13.10.5)
6. Aerial Photogrammetry Survey
7. Global Position System (GPS) Survey (Fig. 13.10.6).

In consideration of time and accuracy, a total electronic station or GPS system is recommended for a subsidence survey. Both the total station and GPS system can determine the elevation and coordinates of the target monument all at once, except that with a total station, the base coordinate and the height of equipment and prism must be known.

Aerial photogrammetry is used frequently in very remote areas, especially when the topography is full of mountain ridges and valleys with high relief. However, the accuracy is poor, around 1 ft (0.3 m).

**Fig. 13.10.4 Auto level**

Fig. 13.10.5 Robotic total station

Fig. 13.10.6 GPS survey station

### 13.10.4 Survey Frequency and Duration

The initial survey should be performed when the mining is about 0.3-0.5 times the cover depth to the area of interest. More lead time should be used when the surface slope is larger than 15% (8.5$^{o}$).

If the area of interest is near the panel setup entry, frequency of surveys should be increased when the face is near the subsidence initiation distance from the panel setup entry and during the active subsidence period of the point of interest, i.e., from 0.1 times the cover depth in advance of the longwall face to one cover depth after passage of the face. Final surveys should be performed when the face has passed the point of interest more than 1.5 times the cover depth.

Longer duration should be planned for residual subsidence and long-term subsidence monitoring.

### 13.10.5 Subsidence Data Processing

Subsidence data processing begins with the determination of surface movement from the raw data obtained from the subsidence survey. It should be noted that some instrumental and human error could be contained in the survey data. Proper techniques should be applied to recognize and eliminate such errors and to produce more accurate monument data. In order to better utilize the subsidence data, reliable deformations should be calculated from the movement data. Again care should be exercised to use proper numerical methods to derive the needed deformations.

## 13.11 SUBSIDENCE INFLUENCES, ASSESSMENT, AND MITIGATIONS

### 13.11.1 Introduction

Surface subsidence causes damages to land and surface structures in critical areas with respect to underground mining configurations such as longwall panels. Damages are represented in the form of ground cracks in the high tension zone (Fig. 13.11.1), bumps in the high compression zone (Fig. 13.11.2), stepped cracks in buildings (Fig. 13.11.3), damage to bridges and linear structures (roads, highways, railroads, pipelines, high voltage power transmission lines, etc.), causing integrity and stability problems to tall structures (silos, water towers, power transmission towers, and transmission towers for TV, radio, and telecommunications) and leakage of water bodies (dewatering of springs, wells, streams, and underground aquifers), and alteration of the landscape (depression zones in large flat area, water pools along streams).

**Fig. 13.11.1 Ground crack formed over a longwall panel**

**Fig. 13.11.2 Bump on an interstate highway formed over the central portion of a longwall panel**

**Fig. 13.11.3 Step cracks on the basement wall of a residential house**

### 13.11.2 Problems Caused by Ground Movements and Deformations

As stated previously, surface subsidence induces vertical subsidence and horizontal displacement. In areas such as the flat bottom areas of a supercritical movement basin where uniform vertical subsidence and horizontal displacement occur, no damage to land and surface structures is expected after mining. Problems show up in areas where differential vertical subsidence and horizontal displacement occurs between adjacent points. The larger the difference, the more severe the problems will be.

Uniform subsidence has very little impact on common structures. But lowering of the land surface may cause water bodies to pond or even flood, it may disturb railroads and bridges making them unstable; and it may reduce effective water flow for rivers. Uniform horizontal displacement, just like uniform vertical subsidence, has little impact on common structures. However, the magnitude of horizontal displacement may damage telephone, power, and pipe lines.

Slope is the difference in vertical subsidence between two adjacent points. Slope will affect slope-sensitive structures and transportation systems, including stability of tall and slender structures (e.g., chimneys, silos, and towers), domestic plumbing systems, drainage systems, and railroads in which the designed maximum grade is 0.7%. Slope may form water ponds if subsidence-induced slope is larger than the natural surface slope. When a residence floor is subject to 1 % or more slope, it is uncomfortable to live in the house.

Horizontal strain is the most critical component for most common structures, especially tensile strain. Strain-induced damages are mainly due to direct contact between the surface structures and the ground. Cracks will occur if the following critical strains are induced on the following structures:

| | |
|---|---|
| Soil | $1.2 \times 10^{-2}$ |
| Asphalt paved surface | $1.0 \times 10^{-2}$ |
| Residential Foundation and basement walls | $3 \times 10^{-3}$ |
| Stone | $3 \times 10^{-3}$ |
| Brick and concrete blocks | $2 \times 10^{-3}$ |

Buried pipelines - strain contributes about 80% to 90% of the stress on the pipelines with rigid joints.

Tall and large dimension structures are very sensitive to curvature, because the magnitude of curvature is proportional to the height of the structure. Ground curvature is the second largest contributor to stress on pipelines with rigid joints. For residential super-structures, problems such as sliding doors and windows, hairline cracks will occur when curvature is equal to or exceeds $6 \times 10^{-5}$ $ft^{-1}$. Large dimension structures are also sensitive to both twisting and shearing.

### 13.11.3 Assessment of Subsidence Influences

In order to select and design proper mitigation measures for subsidence-induced damage, assessment of subsidence influence must be performed to determine the location and severity of damage to the surface structures. Subsidence influence assessment consists of the following steps and guidelines (Luo, 2008)

1. Prediction of surface dynamics and final movements and deformations in and around the structures of interest. At the minimum, subsidence and deformation prediction should be performed along the principal direction of the structures and other directions of interest.
2. The effects of steep surface topography including saturated ground and toe of slope, if they exist, must be considered.
3. The major means of transmission of surface movements and deformations from the surrounding ground to the structures must be determined, looking for the weakest components of the structures.
4. Assessment of structural integrity must be performed (e.g., sources of stresses, stresses on the structure versus strength or critical deformations for the structures).
5. Assessment of structural short term stability (e.g., location of center of gravity after final subsidence) and long term stability (e.g., for high and tall structures, determine the maximum wind force in the direction of the principal slope) must be performed.
6. Assessment of structural functionality (e.g., it is uncomfortable to live if the house floor is tilted more than 1%).

## 13.12 SUBSIDENCE MITIGATIONS

### 13.12.1 Introduction

Numerous case studies have demonstrated (Peng et al., 1995d; Luo et al., 2003) that ground subsidence may cause problems to various surface structures in terms of integrity, stability, and functionality. Surface deformations, in particular tensile strain, are responsible for most subsidence induced damages.

Several methods are available to avoid or reduce subsidence-induced damages to land and surface structures.

### 13.12.2 Methods of Reducing Subsidence Influence

**1. New Structures**

A. Avoid building structures in subsidence-prone areas, such as abandoned mined land or active mining areas (present and future).

B. Employ techniques (e.g., flexible foundation) that will reduce transmission of deformations from the ground to structures.
C. Employ techniques that will strengthen the structure to tolerate deformations expected during mining.

**2. Existing Structures**

A. Underground mine workings can be laid out such that the induced surface movement and deformation in the area of structures is within the tolerable limits of the structures.
B. Avoid placing the surface structures in or within (a) the major influence zone, especially areas of maximum final tensile and compressive strains as well as maximum slope, and (b) the angle of draw.
C. Place structures over the chain pillar system or the flat bottom portion of the super - critical subsidence basins.
D. Employ techniques that will reduce deformations transmitted from ground to structures such that the structures would not be damaged.
E. Strengthen the structures so that they are more tolerable to the deformations imposed upon them.
F. When under the structures of interest, the longwall face should be kept moving as fast as possible to reduce peak dynamic deformations, particularly the maximum dynamic tensile strain. It must be noted that U.S. experience shows that a faster face advancing speed reduces surface structural damages, which is in complete opposition to German experience in that a slower speed is mandated under surface structures to reduce damages (Y Jiang, 2006; Luo et al., 2001a); and that maximum tensile strain is located inside the panel edge, as opposed to outside the panel edge in China.
G. Mining away from the surface slope direction to avoid superposition of slope effect.

### 13.12.3 Support Pillars for Subsidence Mitigation

Current federal regulations prohibit mining under certain protected structures, including structures of vital importance, historic sites, and large public facilities (schools, hospitals, churches, and cemeteries) (U.S. Congress, 1977b). For other types of surface structures, partial mining is allowed. The state of Pennsylvania also prohibits total extraction mining if the overburden depth is less than 100 ft (30.5 m).

**1. Partial Mining**

The most commonly adopted partial room-and-pillar mining plan under surface structures is shown in Fig. 13.12.1 (Gray and Meyer, 1970). A rectangular area of coal (support area) is left below the structure to be protected. This support area is defined by extending the edges of the surface structure by 15 ft (4.6 m) on all sides. Along the edges, a $15^o$ projection line is drawn downward until it reaches the coal seam level. The area enclosed by the projected planes on all sides is the support area. Inside this support area, only partial mining, up to 50% extraction is allowed. Additional offset distance is added on the down slope side if the natural slope is larger than $5^o$.

As mining depth increases, the support area shown in Fig. 13.12.1 will be excessively large, resulting in a waste of coal reserves. In addition, the effect of mining height is not considered in this method.

To overcome the shortcomings of the method shown in Fig. 13.12.1, Peng and Luo (1994) proposed a new method to define the support area. In this method, the subsidence

prediction method discussed in Section 13.4.3 is used to determine the site specific-surface movement and deformation in and around surface structures. The critical deformation indices (i.e., slope, strain, and curvature) are then used to assess damage potential to the structures. As a result, different offsets are recommended for different structures, and different critical deformation values are applied to different structural types (Fig. 13.12.2 and Table 13.12.1).

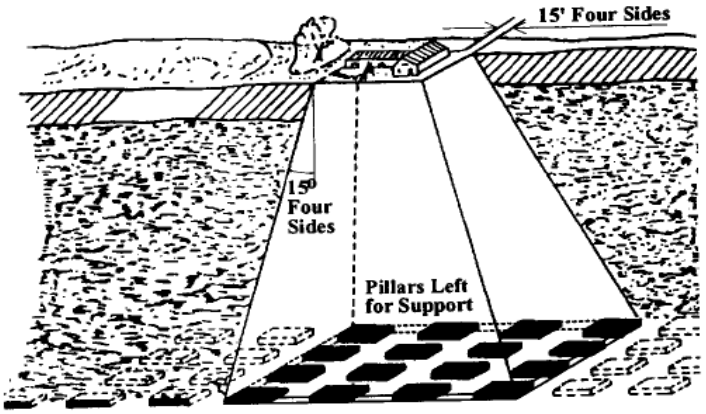


**Fig. 13.12.1 Method of supporting surface structures (Gray and Meyer, 1970)**

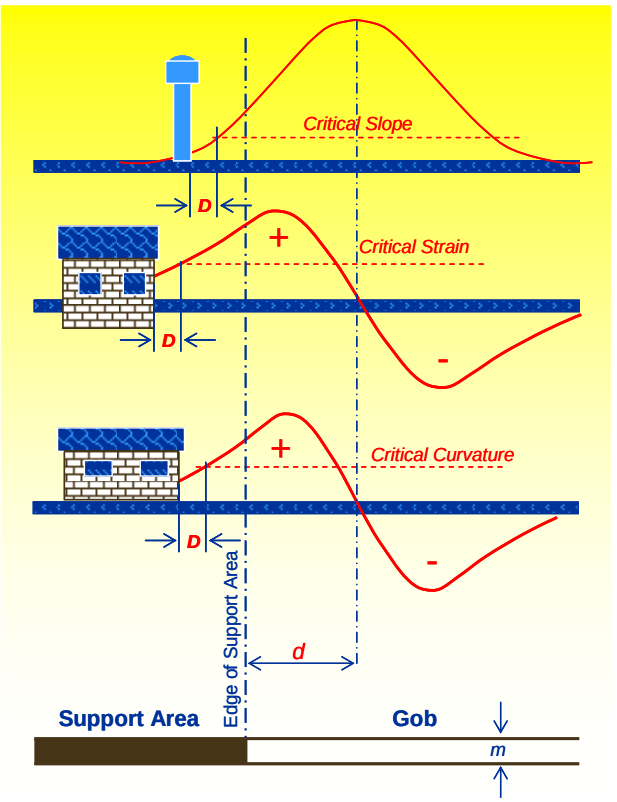


**Fig. 13.12.2 Design principles for a new support area (Peng and Luo, 1994)**

**Table 13.12.1 Recommended offset distance (Peng and Luo, 1994)**

| Class | Type of structure | Offset distance, ft |
|---|---|---|
| I | High voltage (>220 KV) power transmission towers, power transformer stations, highway bridges, coal storage silos, hospitals, schools, buildings of more than three stories, radio and television transmission towers, historical structures, railway or mass transit stations, main structure of power generation plants and main surface facilities, etc. | 45 |
| II | Brick residential houses, power transmission towers (<220 KV), etc. | 30 |
| III | Wood-frame residential houses, simple storage silos, temporary structures, etc. | 15 |

**2. Panel Design Considerations**

A. Locate structures over gateroads or mains and bleeder chain pillar systems.
B. Locate structures on the flat bottom part of the final subsidence basin for super-critical conditions.
C. Orient the panel longitudinal direction such that structural width is parallel to the maximum principal strain.
D. Use as wide a panel as possible to reduce the total area of major influence or increase the flat bottom area.
E. Use the yield chain pillar system when overburden is large to produce large and relatively mild overall subsidence basins.

### 13.12.4 Mitigation Measures

For various types of surface structures commonly found in all U.S. coalfields, the following simple and easily-implementable techniques have proven to be highly effective (Luo et al., 2003).

**1. Residential Structures (Fig. 13.12.3)**

**A. Compensation trench**

A **Compensation trench** is a channel dug around a house, 3-6 ft (0.9-1.8 m) from the exterior wall of the house, 2 ft (0.6 m) wide, and to a depth 2 ft (0.61 m) or more below the foundation (Dutta et al., 1993; Peng, 1992). This trench is designed to reduce the severity of disturbance to structural parts that are in direct contact with the ground. A compensation trench creates a weak plane between the structure and the ground so that a reduction of surface strain transmission from the ground to the structure can be achieved. Knowing the location where the strain is generated is important to correctly use this method. The compensation trench is more effective in reducing compressive strain (up to 65% reduction in recorded case studies) than tensile strain (35% reduction recorded).

**B. Leveling method**

Leveling is designed to reduce the severity of disturbance to a super-structure. In this method the super-structure is kept on a level plane all the time during the dynamic subsidence process.

However, the needed adjustment could be impractically large. When the mine is shallow, the required adjustment could actually create more artificial damage than the subsidence process.

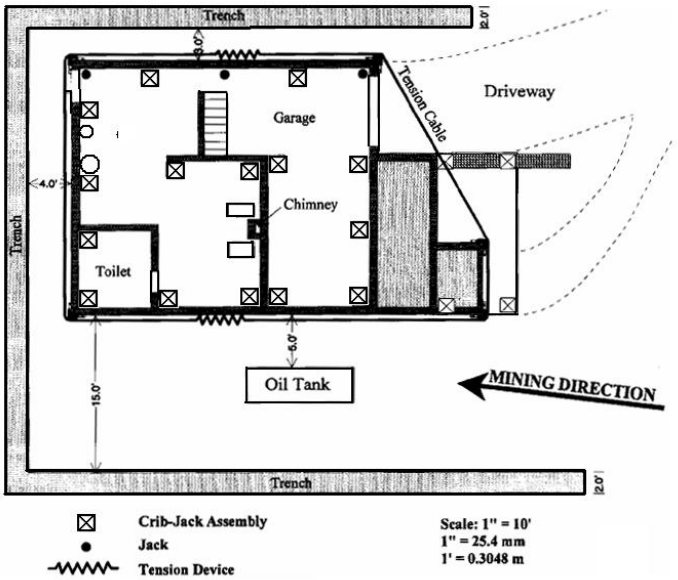


**Fig. 13.12.3 Compensation trench, tension cable, and plane-fitting methods used for a residential structure to mitigate the intensive dynamic subsidence effects over a shallow longwall mine (Luo, 2008)**

### C. Plane-fitting method

This subsidence mitigation method is also designed to reduce the severity of disturbance to a super-structure. The super-structure is kept on a time-dependent inclined plane so that it is free of stress caused by the bending and twisting actions associated with the ground subsidence process. In determining the desired inclined plane at a given time, the total amount of required adjustment should be minimized in order to keep any damage resulting from the adjustment operation itself as small as possible. A method has been developed to determine the optimum inclined plane at any instant (Luo et al., 1992).

### D. Tension cable method

This method is suitable for structures that have relatively high compressive strength, such as stone, block, and brick structures. It can reduce damage caused by twisting and bending actions and prevent crack propagation.

In this method the structure to be protected is wrapped with one or more pre-tensioned steel wire cables. It can serve the following two purposes:

1. The tension force applied by the cables places the structure into a compression state so that it is able to compensate some of the subsidence-induced final or dynamic tensile stresses, and
2. The rigidity of those structural parts is increased so that they can tolerate more deformations transmitted to them.

The minimum amount of pre-tension required to prevent splitting of a structure by curvature can be determined by (Fig. 13.12.4) (Luo et al., 1992).

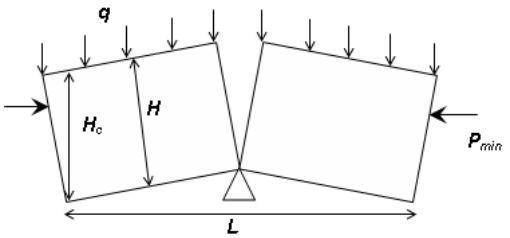


**Fig. 13.12.4 Symbols for tension cable method (Luo, 2008)**

$$P_{\min} = \frac{L^2}{8H_c}\left(q + Hb\gamma\right) \tag{13.12.1}$$

where $q$ is roof load on the wall, $b$ is thickness of the wall, $\gamma$ is specific weight of the wall material, $H$ is the height of the wall, and $H_c$ is location of the cable above the ground.

**E. External/Internal Bracing**

Wood materials are used to enhance weak spots (e.g., doors, windows, and indent parts) of the structure.

**F. Slotting**

A large structure is subjected to larger differential deformation than a smaller structure. By dividing a large structure into smaller units through slotting, damage to a large structure can be avoided. Slotting is best suitable for large concrete or asphalt pavement subject to both tensile and compressive strains.

For tensile strain, a thin slot, without cutting through the thickness of the pavement, should be made perpendicular to the direction of the principal strain. For compressive strain, the width of the slots should be properly determined as follows,

$$W_{slot} = \varepsilon_{max} \text{ x } L_{block} \tag{13.12.2}$$

where $\varepsilon_{max}$ is the maximum compressive strain anticipated, and $L_{block}$ is the length of the block between slots. In case of roadways, the slots should be cut through the thickness of the pavement so that any potential bump can be avoided.

## 13.13 FINAL SUBSIDENCE OVER IRREGULAR MINE OPENINGS

A large non-rectangular underground mine gob formed by mining operations, such as pillar retreating operation in a room and pillar coal mine, could also induce surface subsidence. Zone area method is used to predict final subsidence in such case (Luo et al., 2008). This method is based on the fact that the extraction at a location more than one $R$ away from the prediction point offers very little influence to that surface point. Therefore, only the influences caused by extraction within $R$ distance from the prediction point (the major influence zone) and the computing boundary are counted as shown in Fig. 13.13.1. The major influence zone is subdivided into a number of sub-zones. The subsidence contribution for each of the sub-zones can be pre-calculated. If the major influence zone is equally divided into $N$ rings and $M$ sectors, a subzone $C(i,j)$ located in the computing boundary will contribute $S_{\max} \times W_{i,j}$ amount to the final subsidence at a surface point $(x, y)$. Subscripts $i$ and $j$ represent the ring and sector that a subzone is located, respectively. Weighting factor for this subzone $W_{i,j}$, also equal to the other subzone in the $i$th ring $W_i$, can be determined by Eq. 13.13.1, in which $C_c$ is a correction

factor to compensate the minor error due to the exclusion of the influence beyond the major influence zone and is determined to be 1.0452.

$$W_{i,j} = W_i = \frac{C_c}{M}\left[ e^{-\pi\left(\frac{i-1}{N}\right)^2} - e^{-\pi\left(\frac{i}{N}\right)^2} \right] \quad i = 1, 2, \ldots.N \tag{13.13.1}$$

where $M$ is mining height.

To predict the final subsidence at point (x, y), the center of the subdivided major influence zone is placed at the prediction point. Then the number of sub-zones that are enclosed in the computing area is counted and the final subsidence at the prediction point is calculated by summing the total influences as shown by Eq. 13.13.2, in which, $n_i$ is the number of cells in $i$th ring that are enclosed by the computing boundary (Fig. 13.13.2).

$$S(x,y) = S_{\max} \sum_{i=1}^{N} \sum_{j=1}^{M} W_{i,j} = S_{\max} \sum_{i=1}^{N} \left(n_1 W_i\right) \tag{13.13.2}$$

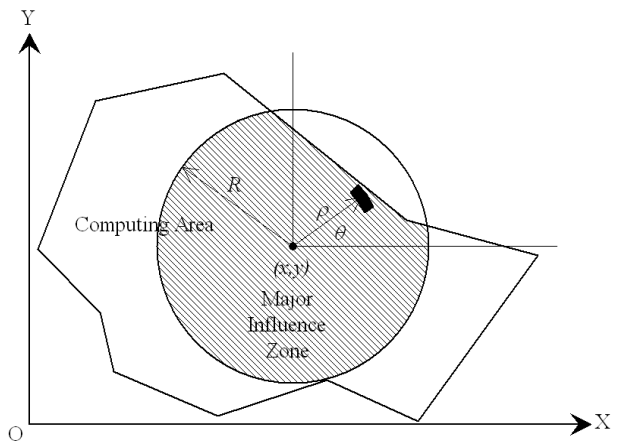


**Fig.13.13.1 Zone Area Method in predicting final subsidence over irregular mine openings (Luo et al., 2008)**

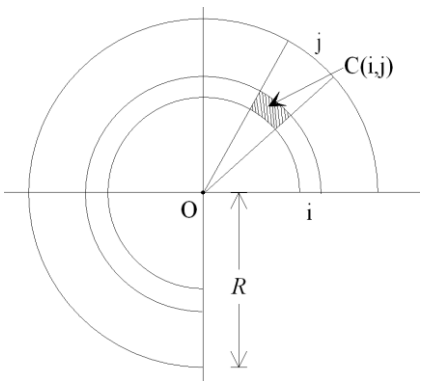


**Fig. 13.13.2 Determining weighting factor for subzone C (i, j) (Luo et al., 2008)**